Doctoral Dissertation

Studies on Cellulose Nanofiber Reinforced Starch Films with Water Durability and Marine Degradability

（耐水性と海洋生分解性を有するセルロースナノ繊維強化デンプンフィルムに関する研究）

RAGHAV SONI

July 2021

Graduate School of Engineering,

Osaka University

Contents

List of Abbreviations

AOS	Acetyl oxidized starch
AS	Acetyl starch
Di-aldS	Di-aldehyde starch
DNPH	2,4-dinitrophenylhydrazine
HPS	Hydroxypropyl starch
MCNF	Mechanically fibrillated cellulose nanofiber
NTS	Native tapioca starch
OMCNF	Oxidized mechanically fibrillated cellulose nanofiber
PE	Polyethylene
PCL	Poly(ε-caprolactone)
PLA	Polylactic acid
PP	Polypropylene
PS	Polystyrene
PVC	Polyvinyl chloride
R-TCNF	Reduced-TEMPO oxidized cellulose nanofiber
TCNF	TEMPO-oxidized cellulose nanofiber
TEMPO	2,2,6,6-Tetramethylpiperidin-1-yl)oxyl
WUR	Water uptake ratio

General introduction

Plastic packaging is essential for preserving, protecting, processing, and transporting food[1]. Numerous petrochemical polymers such as PE, PP, PS, and PVC are extensively used in packaging industries owing to high flexibility, transparency, strength, impermeability, and easy processibility[2]. Anthropogenic littering of petrochemical plastic presents a substantial source of contamination in the intertidal and subtidal benthos[3]. Biodegradable, oxo-biodegradable, and compostable plastic are often regarded as potential solutions to the accumulation of plastic litter and waste. However, certain conditions (as temperature, humidity, light, oxygen demand, CO_2 evolution) are required for the breakdown of the polymer chain[4]. It is found that plastic bags that claim to be biodegradable were still functional as carry bags after 3 years in the marine environment[5]. Biodegradable polymers as PCL, PVL, and Ecoflex (polybutylene adipate terephthalate) were not degradable at all, and PHB degrades only by 9% in seawater[6]. So, there is a lack of evidence that biodegradable, oxo-degradable plastics offer a marine environment advantage over conventional plastics[7]. The potential for fragmentation into micro-plastics causes additional concern[8].

Marine biodegradable plastics have previously been developed with PHA, PHBH, and PBS[9–11]. However, these are both categorized as aliphatic polyesters and are of poor quality compared to conventional plastics, such as polyethylene and polypropylene, while being producible only in low yields (approximately tens of thousands of tons per year compared to an annual global production of 300 million tons for conventional plastics) and at more than twice the cost of that of conventional plastics, all of which are factors that have limited their use[11–13]. Thus, there has been a strong demand for the

development of a low-cost and mass-producible marine biodegradable plastic that can enable us to tackle the growing problem of marine debris[14]. To overcome this problem, biodegradable polymers from renewable resources have attracted much attention as packaging materials of the next generation.

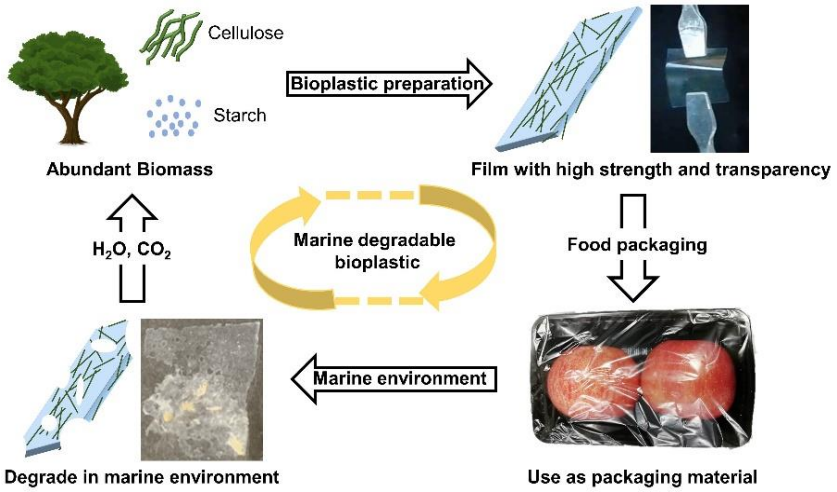

Fig. 1. Concept of polysaccharide based packaging film to reduce marine pollution.

Polysaccharides are the potential substitutes for petrochemical polymers due to their biodegradability and renewability. Cellulose and starch are the amplest biomass[15]. Hydrolysis via the enzymatic route is accomplished synergistically by actions of a group of enzymes known as cellulases and amylase[16]. Marine microbes as isoptericola, bacillus, halomonas, pseudomonas, etc., are potential cellulases and amylase sources[17]. It is found that cellulases/amylase from marine microbes were used to hydrolyze different plant biomasses such as bamboo, cumbu leaf, sorghum. Bacillus cereus showed bioconversion of plant biomass to fermentable sugar[18]. Therefore, packaging bags prepared by biomass (as cellulose and starch) are the potential substitute for

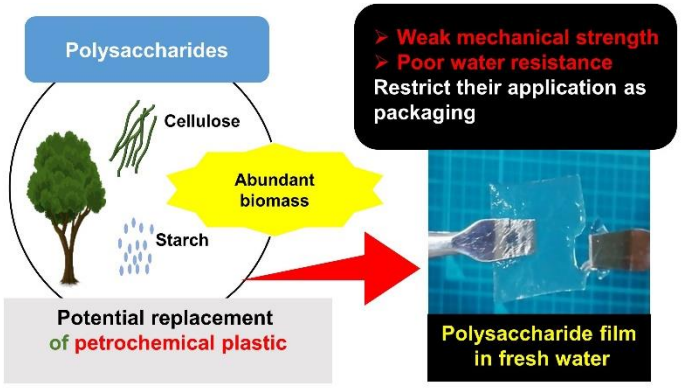

Fig. 2. Presentation of water durability problem associated with polysaccharides films.

low-cost marine compostable single-use plastic (**Fig. 1**). However, the lack of strength and durability of cellulose and starch in freshwater restricts their application (**Fig. 2**)[19,20].

Cellulose is the most abundant occurring natural polymer on earth, being the predominant constituent in cell walls of all plants. Cellulose is composed of a unique monomer: glucose under its β-D-glucopyranose form. Due to its regular structure and array of hydroxyl groups[21], it tents to form strong hydrogen bonded crystalline microfibrils and fibers and is most familiar in the form of paper and paperboard in the packaging context[22]. However, these packaging are opaque, has low mechanical strength and poor water durability.

Many chemically modified celluloses as cellulose acetate, cellulose octanoate, cellulose palmitate, and methylcellulose have been prepared to improve water durability[23,24]. Such hydrophobic modification was found to enhance water durability; however, enzymatic degradation was drastically reduced. Almost zero hydrolysis rate for cellulose acetate, cellulose octanoate, cellulose palmitate by enzymatic degradation has been reported in the earlier study[25,26].

To prepare transparent and high strength packaging film, cellulose is disintegrated into microfibrillated or nanofibrillated cellulose (MFC or NFC) by physical methods (grinding, high pressure homogenizing) or chemical methods (TEMPO-oxidation, oxoammonium salt oxidation etc.)[27–29] (**Fig. 3**). Because of the unique characteristics of MFC and NFC as; a very high surface area, high aspect ratio, high crystallinity, have wide range of applicability in material technology[30,31]. MFC and NFC mostly used as; reinforcement in nanocomposite, filtration media, antimicrobial membranes, and oxygen barrier material in food, cosmetic and pharmaceutical industries[32–34]. MFC and NFC production requires repeated disintegration of the cellulose suspension using a high-pressure homogenizer (physical method), which consumes a huge amount

of energy in large-scale production[35]. Therefore, development of packaging film become costly and not costumer friendly.

NFC production by chemical methods become popular owning to fast, easy and economical processability. 2,2,6,6-tetramethylpiperidine-1-oxyl (TEMPO) is a water-soluble and stable nitroxyl radical, and commercially available for laboratory and industrial use.

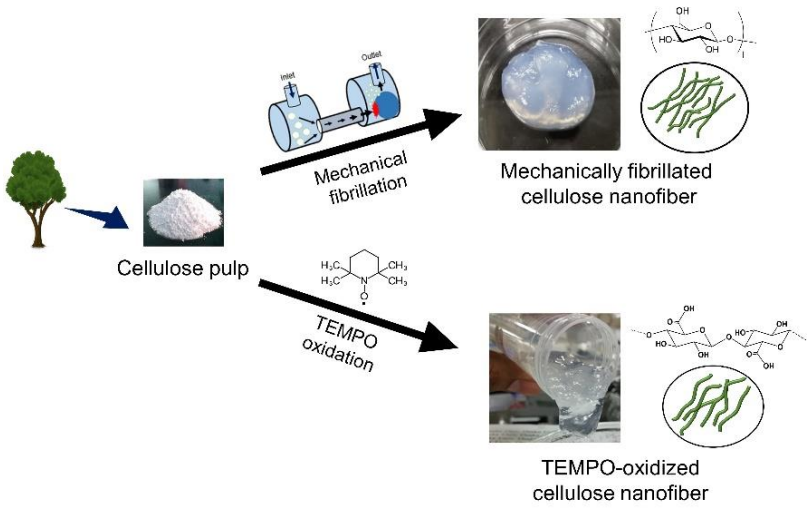

Fig. 3. Illustrative representation of preparation of cellulose nanofiber by (A) mechanically fibrillation method and (B) chemical method (TEMPO-oxidation).

TEMPO-mediated oxidation of cellulose is position-selective oxidation of C6-primary hydroxyl groups to sodium C6-carboxylate groups with a TEMPO/NaBr/NaClO system in water at pH 10.5. After oxidation, the yield is processed by mechanical disintegration (carboxylate moieties created strong electrostatic repulsion) to prepare highly fibrillated TEMPO-oxidized cellulose nanofiber (TCNF)[36,37].

TCNF is used in ultra-low density transparent aerogel preparation with high specific surface area, transparent, strong, and high-oxygen barrier films preparation, water filter preparation to absorb heavy metal ions, bone and cartilage tissue engineering owning to calcium deposition properties, lubricating agents and cosmetic hydrogel etc[38–41]. TCNF film has high optical transparency, mechanical strength and oxygen barrier properties that is make the TCNF film quite suitable for packaging applications.

However, TCNF film has swelling network due to strong electrostatic repulsion among carboxylate moieties. So, TCNF film showed poor water durability owing to microgel structure formation after immersion in water[42]. Many polymers such as poly(acrylamide) (PAM), poly(vinylamine) (PVAm), and poly(ethyleneimine) (PEI) have been introduced to TCNF to further improve its wet tensile strength[43]. However, these synthetic polymers non-degradable are hazardous to the environment.

Starch is a biocompatible, biodegradable, renewable, and abundant polysaccharide. Starch is regenerated from carbon dioxide and water by photosynthesis in plants[44]. Starch is mainly composed of two homopolymers of D-glucose: amylose, a mostly linear α-D(1,4')-glucan and branched amylopectin, having the same backbone structure as amylose but with many α-1,6'-linked branch points. Starch has different properties of amylose and amylopectin ranging from about 10-20% amylose and 80-90% amylopectin depending on the source. Starch occurs naturally as discrete granules since short branched amylopectin chains are able to form helical structure which crystallize[45] (**Fig. 4A**).

In order to prepare film, starch granule suspended in water and followed by gelatinization. When heated in water, starch granules swell, so amylose leaching and partial granule disruption

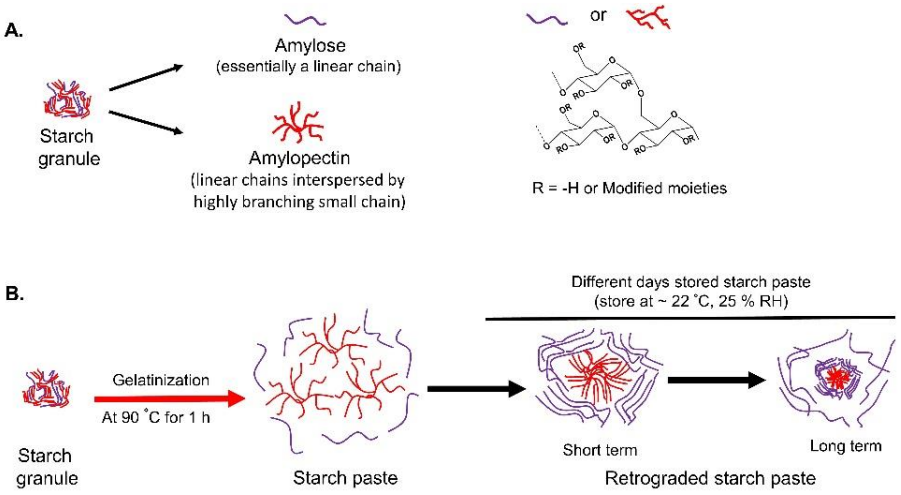

Fig. 4. Representation of (A) starch granule, amylose and amylopectin and (B) starch paste retrogradation process (reassociation of amylose and amylopectin in starch paste during storage).

occur. This process is called the gelatinization of starch[46]. Disruption of the semi-crystalline arrangement requires high energy, so gelatinization of native starch granules is achieved at high temperatures (above 80 °C). The starch paste poured into dish and followed by solvent casting method. The prepared starch film has high optical transparency; however, it is highly brittle and immediately dissolved in water. Therefore, only starch films are not suitable for packaging application[47].

Crystallinity also influence starch film water durability and wet strength. Starch paste crystallinity can be changed by amylose and amylopectin reassociation, the process called retrogradation[48]. Starch granules have an amorphous core (composed of amylose) surrounded by concentric semi-crystalline growth rings alternating with amorphous growth rings (composed of amylose and amylopectin). Gelatinization occurs initially in the amorphous region, loosely bound amylose chain leaches out from the granule and starch granule loss its birefringence and crystalline order. When the starch gel is cooled and stored, disaggregated amylose and amylopectin chains reassociate to form a more ordered structure; this is called starch retrogradation. Retrogradation is an inevitable process for native starch, linear amylose chain reassociates initially during the cooling of the starch paste and formation of ordered or crystalline amylopectin molecules take place during storage (**Fig. 4B**). Higher amylose content starches have rapid retrogradation. Starch retrogradation usually results in an increased degree of crystallinity with the appearance of B-type crystalline polymorphs[49,50]. However, a packaging film cast with only gelatinized starch or retrograded starch has poor wet strength and collapses in water.

Due to potential reactivity of hydroxyl groups, serval chemically modified starch has prepared as hydroxypropyl starch (HPS), acetyl starch (AS), acetyl-oxidized starch (AOS), di-aldehyde starch (Di-aldS), octanyl succinate starch etc[51–53] (**Fig. 5**). Although, chemical modification found

to enhance starch film mechanical properties but water durability is inferior for packaging application. Starch is blended with serval polymers as PE, PVA, PLA, PCL, PHA etc. Starch blend composites showed good mechanical properties and adequate degradability, however, compatibility between hydrophilic and hydrophobic polymer, and use of urea and formamide are point of concerns[54–57].

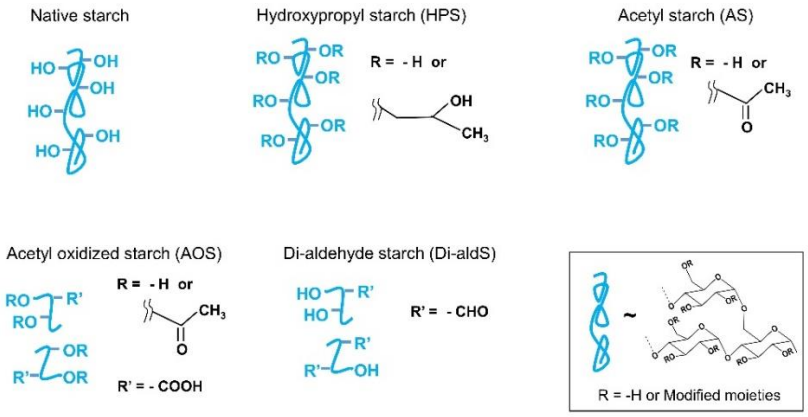

Fig. 5. Physiochemical structure of differently modified starches.

In this thesis, the author has proposed a starch crosslinker to enhance mechanical properties, and water durability of cellulose nanofiber reinforced starch film. The blending of starch with oxidized cellulose nanofiber in the optimized concentration was found to improve film properties. The formation of hemiacetal crosslinking between hydroxyl groups of starch and aldehyde groups of oxidized cellulose has a crucial role in elevated water durability. Further, comprehensively analyzed the role of different kinds of starches as HPS, AS, AOS, Di-aldS, and differently oxidized cellulose nanofibers as TEMPO-oxidized, sodium periodate oxidized, sodium bromide oxidized. Moreover, starch paste crystallinity was optimized to synergize crystallization and hemiacetal crosslinking to enhance film properties. In addition, enzymatic degradation and marine microbial degradation were analyzed to confirm the degradability of the films. Therefore, starch crosslinker

elevated the film properties and increased the microbial degradability of the films. This thesis is composed of 3 chapters as

In chapter 1, the formation of hemiacetal crosslinking between starch and cellulose nanofiber has studied. TEMPO-oxidized cellulose nanofiber (TCNF) was blended with three different types of modified starch: hydroxypropyl starch (HPS), acetyl starch (AS), and acetyl oxidized starch (AOS), respectively. It was demonstrated that the TCNF/starch film exhibited reduced swelling in water and enhanced mechanical strength in wet condition compared to neat TCNF or starch film because hemiacetal bonding was formed between TCNF and starch (**Fig. 6**). Thus, the formation of hemiacetal crosslinking has a dominating role in elevate water durability of TCNF/starch film.

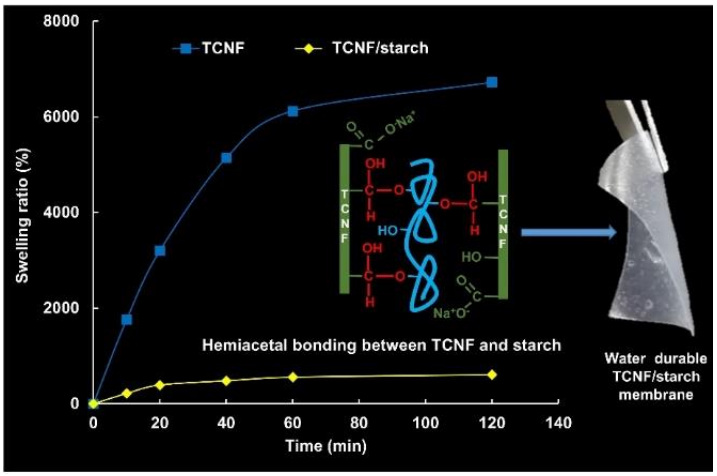

Fig. 6. Graphical presentation of swelling reduction in TCNF/starch film owing to hemiacetal crosslinking formation.

In chapter 2, synergistic effect to starch paste crystallinity and hemiacetal crosslinking has studied. TCNF/starch films prepared by mixing different-storage-duration native tapioca starch (NTS), hydroxypropyl starch (HPS), and di-aldehyde starch (Di-aldS) with TCNF.

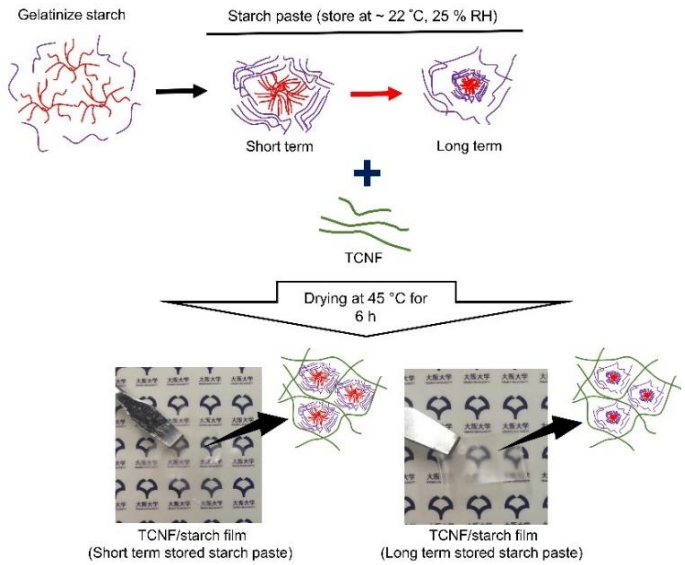

Fig. 7. TCNF/starch film prepared with short-term and long-term stored starch paste, and corresponding TCNF, amylose and amylopectin arrangement.

We demonstrate that the films prepared with the stored starch pastes exhibit improved mechanical properties and wet strength owing to the synergistic effect of enhanced crystallinity and hemiacetal crosslinking. However, long-term storage of the starch pastes negatively affected their properties (**Fig. 7**).

In chapter 3, we used a wet pulverization process to prepare mechanically fibrillated cellulose nanofiber (MCNF). They were further followed by sodium periodate oxidation to prepare oxidized cellulose nanofiber (OMCNF). MCNF and OMCNF were converted into a film by a solvent casting process. OMCNF film prepared with 1 h oxidized cellulose nanofiber had significantly higher wet tensile strength than MCNF film. Also, water durability can further be enhanced by adding starch (Hydroxypropyl starch, HPS) with OMCNF. Moreover, starch addition enhanced microbial growth that increased the degradability of OMCNF/HPS film in marine conditions. Thus, OMCNF/HPS film had adequate freshwater durability with marine degradability (**Fig. 8**) and has the potential to serve as next-generation packaging material.

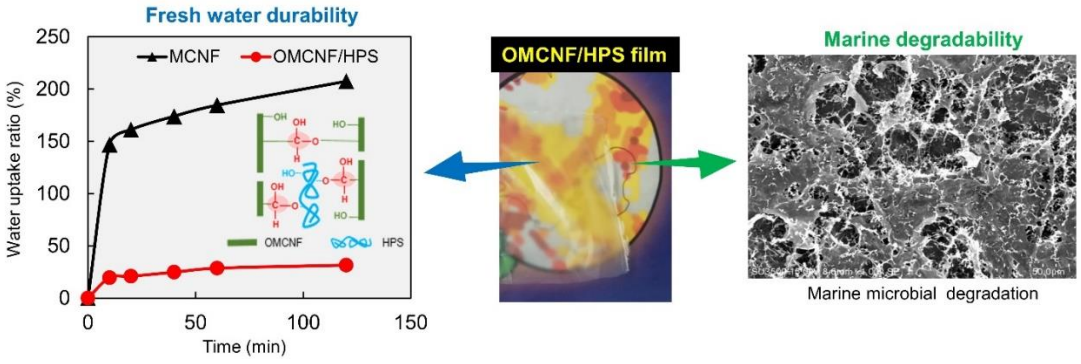

Fig. 8. Cellulose nanofiber reinforced starch film possess high fresh water durability and adequate marine degradability.

References

(1) Ferreira, A.; Alves, V.; Coelhoso, I. *Membranes (Basel).* **2016**, *6* (2), 22.

(2) Rahimi, A.; García, J. M. *Nat. Rev. Chem.* **2017**, *1* (6), 0046.

(3) Rech, S.; Borrell Pichs, Y. J.; García-Vazquez, E. *PLoS One* **2018**, *13* (1), e0191859.

(4) Chamas, A.; Moon, H.; Zheng, J.; Qiu, Y.; Tabassum, T.; Jang, J. H.; Abu-Omar, M.; Scott, S. L.; Suh, S. *ACS Sustain. Chem. Eng.* **2020**, *8* (9), 3494–3511.

(5) Napper, I. E.; Thompson, R. C. *Environ. Sci. Technol.* **2019**, *53* (9), 4775–4783.

(6) Bagheri, A. R.; Laforsch, C.; Greiner, A.; Agarwal, S. *Glob. Challenges* **2017**, *1* (4), 1700048.

(7) Thomas, N. L.; Clarke, J.; McLauchlin, A. R.; Patrick, S. G. *Waste and Resource Management*. August 1, **2012**, pp 133–140.

(8) Mateos-Cárdenas, A.; O'Halloran, J.; van Pelt, F. N. A. M. *Sci. Rep.* **2020**, *10* (1), 12799.

(9) Delamarche, E.; Mattlet, A.; Livi, S.; Gérard, J. F.; Bayard, R.; Massardier, V. *Front. Mater.* **2020**, *7* (7), 7.

(10) Dilkes-Hoffman, L. S.; Lant, P. A.; Laycock, B.; Pratt, S. *Mar. Pollut. Bull.* **2019**, *142*, 15–24.

(11) Suzuki, M.; Tachibana, Y.; Kasuya, K. ichi. *Polymer Journal*. Springer Nature, **2021**, pp 47–66.

(12) Wen, Q.; Chen, Z.; Tian, T.; Chen, W. *J. Environ. Sci.* **2010**, *22* (10), 1602–1607.

(13) Li, D.; Fu, J.; Ma, X. *Polym. Compos.* **2020**, *41* (1), 381–390.

(14) Luckachan, G. E.; Pillai, C. K. S. *J. Polym. Environ.* **2011**, *19* (3), 637–676.

(15) Song, J. H.; Murphy, R. J.; Narayan, R.; Davies, G. B. H. *Philos. Trans. R. Soc. B Biol. Sci.* **2009**, *364* (1526), 2127–2139.

(16) Carrasco, M.; Villarreal, P.; Barahona, S.; Alcaíno, J.; Cifuentes, V.; Baeza, M. *BMC Microbiol.* **2016**, *16* (1), 1–9.

(17) Trivedi, N.; Reddy, C. R. K.; Lali, A. M. In *Advances in Food and Nutrition Research*; Academic Press Inc., **2016**; Vol. 79, pp 27–41.

(18) Annamalai, N.; Thavasi, R.; Vijayalakshmi, S.; Balasubramanian, T. *Indian J. Microbiol.* **2011**, *51* (4), 424–429.

(19) Müller, C. M. O.; Laurindo, J. B.; Yamashita, F. *Food Hydrocoll.* **2009**, *23* (5), 1328–1333.

(20) Niranjana Prabhu, T.; Prashantha, K. *Polym. Compos.* **2018**, *39* (7), 2499–2522.

(21) Fernandes, A. N.; Thomas, L. H.; Altaner, C. M.; Callow, P.; Forsyth, V. T.; Apperley, D. C.; Kennedy, C. J.; Jarvis, M. PNAS, **2011**, 108 (47), E1195-E1203.

(22) Cruz-Romero, M.; Kerry, J. P. *CAB Reviews, Perspectives in Agriculture, Veterinary Science, Nutrition and Natural Resources*, **2008**.

(23) Tanaka, S.; Iwata, T.; Iji, M. *ACS Sustain. Chem. Eng.* **2017**, *5* (2), 1485–1493.

(24) Mikaeili, F.; Gouma, P. I. *Sci. Rep.* **2018**, *8* (1), 1–8.

(25) Leppänen, I.; Vikman, M.; Harlin, A.; Orelma, H. *J. Polym. Environ.* **2020**, *28* (2), 458–470.

(26) Puls, J.; Wilson, S. A.; Hölter, D. *Journal of Polymers and the Environment*, **2011**, pp 152–

165.

(27) Levanič, J.; Šenk, V. P.; Nadrah, P.; Poljanšek, I.; Oven, P.; Haapala, A. *ACS Sustain. Chem. Eng.* **2020**, *8* (48), 17752–17762.

(28) Isogai, A.; Hänninen, T.; Fujisawa, S.; Saito, T. *Progress in Polymer Science*, **2018**, pp 122–148.

(29) Kargarzadeh, H.; Mariano, M.; Gopakumar, D.; Ahmad, I.; Thomas, S.; Dufresne, A.; Huang, J.; Lin, N. *Cellulose*, **2018**, pp 2151–2189.

(30) Mishra, R. K.; Sabu, A.; Tiwari, S. K. *Journal of Saudi Chemical Society*, **2018**, pp 949–978.

(31) Osong, S. H.; Norgren, S.; Engstrand, P. *Cellulose*, **2016**, pp 93–123.

(32) Dufresne, A. *Philosophical Transactions of the Royal Society A: Mathematical, Physical and Engineering Sciences*, 2018.

(33) Nechita, P.; Iana-Roman, M. R. *Coatings*. MDPI AG, **2020**, p 566.

(34) Sharma, A.; Thakur, M.; Bhattacharya, M.; Mandal, T.; Goswami, S. *Biotechnology Reports*, **2019**, p e00316.

(35) Xie, H.; Du, H.; Yang, X.; Si, C. *International Journal of Polymer Science*, **2018**.

(36) Isogai, A. *Jpn. Acad. Ser. B. Phys. Biol. Sci.* **2018**, *94* (4), 161–179.

(37) Isogai, A.; Saito, T.; Fukuzumi, H. *Nanoscale* **2011**, *3* (1), 71–85.

(38) Isogai, A. *Proceedings of the Japan Academy Series B: Physical and Biological Sciences*. Japan, **2018**, pp 161–179.

(39) Wang, M.; Shao, C.; Zhou, S.; Yang, J.; Xu, F. *RSC Adv.* **2017**, *7* (61), 38220–38230.

(40) Fukuzumi, H.; Saito, T.; Iwata, T.; Kumamoto, Y.; Isogai, A. *Biomacromolecules* **2009**, *10* (1), 162–165.

(41) Al-Ahmed, Z. A.; Hassan, A. A.; El-Khouly, S. M.; El-Shafey, S. E. *Polym. Bull.* **2020**, *77* (12), 6213–6226.

(42) Maloney, T. C. *Holzforschung* **2015**, *69* (2), 207–213.

(43) Miao C, Leduc M, Pelton R. *Journal of Pulp and Paper Science*, **2008**, 34(1), 69.

(44) Lu, D. R.; Xiao, C. M.; Xu, S. J. *Express Polym. Lett.* **2009**, *3* (6), 366–375.

(45) Rolland-Sabaté, A.; Sánchez, T.; Buléon, A.; Colonna, P.; Jaillais, B.; Ceballos, H.; Dufour, D. *Food Hydrocoll.* **2012**, *27* (1), 161–174.

(46) Cornejo-Ramírez, Y. I.; Martínez-Cruz, O.; Del Toro-Sánchez, C. L.; Wong-Corral, F. J.; Borboa-Flores, J.; Cinco-Moroyoqui, F. J. *CyTA - J. Food* **2018**, *16* (1), 1003–1017.

(47) Ribba, L.; Garcia, N. L.; D'Accorso, N.; Goyanes, S. In *Starch-Based Materials in Food Packaging: Processing, Characterization and Applications*, **2017**; pp 37–76.

(48) Wang, S.; Li, C.; Copeland, L.; Niu, Q.; Wang, S. *Compr. Rev. Food Sci. Food Saf.* **2015**, *14* (5), 568–585.

(49) Miles, M. J.; Morris, V. J.; Orford, P. D.; Ring, S. G. *Carbohydr. Res.* **1985**, *135* (2), 271–281.

(50) Zhang, Y.; Liu, W.; Liu, C.; Luo, S.; Li, T.; Liu, Y.; Wu, D.; Zuo, Y. *Food Chem.* **2014**, *158*, 255–261.

(51) Fu, Z.; Zhang, L.; Ren, M.-H.; BeMiller, J. N. *Starch*, **2019**, *71* (1–2), 1800167.

(52) Fonseca, L. M.; Gonçalves, J. R.; El Halal, S. L. M.; Pinto, V. Z.; Dias, A. R. G.; Jacques, A. C.; Zavareze, E. da R. *LWT - Food Sci. Technol.* **2015**, *60* (2), 714–720.

(53) Lawal, O. S. *Carbohydr. Res.* **2004**, *339* (16), 2673–2682.

(54) H i Niu X, Ma Q, Li S, Wang W, Ma Y, Zhao H, Sun J, Wang J. *Journal of Food Quality*. **2021**.

(55) Liu, W.; Chen, Y.; Ouyang, L.; Liu, Y.; Hao, X. *Advanced Materials Research*; **2012**, 496,134–137.

(56) Begum, M. H. A.; Hossain, M. M.; Gafur, M. A.; Kabir, A. N. M. H.; Tanvir, N. I.; Molla, M. R. *SN Appl. Sci.* **2019**, *1* (9), 1–9.

(57) Pirooz, M.; Navarchian, A. H.; Emtiazi, G. *J. Polym. Environ.* **2018**, *26* (4), 1702–1714.

Chapter 1

Cellulose nanofiber reinforced starch film with high mechanical strength and water durability

1.1 Introduction

Cellulose is the amplest biomass on the earth. In the production of transparent packaging membranes, cellulose fibers are disintegrated in micro/nano sized fibers, so called microfibrillated cellulose (MFC). MFC production requires repeated disintegration of the cellulose suspension using a high-pressure homogenizer, which consumes a huge amount of energy in large scale production[1].

TEMPO-mediated oxidation converts the C6 primary alcohol of cellulose into carboxylic acid. Electrostatic repulsion among the carboxylate moieties liberates the cellulose nanofiber in water, producing TEMPO-oxidized cellulose nanofiber (TCNF)[2]. TCNF has a high crystallinity (~74%), and high aspect ratio (4-20 nm wide, 500-2000 nm length). TCNF self-standing membrane is flexible and transparent with a high tensile modulus (6-7 GPa). Therefore, the TCNF membrane is a suitable packaging material[3]. However, its poor wet strength and swelling network restrict many packaging applications. In wet TCNF membrane, anionically charged microfibrils generate strong electrostatic repulsion, which disturbs its fiber arrangement and allows water to permeate into the network[4].

Some aldehyde moieties form as intermediate structures on the cellulose microfibrils during the TEMPO-mediated oxidation. It is reported that intermediate aldehyde moieties significantly contribute to improving the TCNF membrane wet strength by hemiacetal linkage formation[5,6].

Many polymers such as poly(acrylamide) (PAM), poly(vinylamine) (PVAm), and poly(ethyleneimine) (PEI) have been introduced to TCNF to further improve its wet tensile strength[7]. However, these synthetic polymers are hazardous to the environment. On the other hand, starch is biocompatible, biodegradable, renewable, and is an abundant polysaccharide[8]. Presence of hydroxyl groups make it a suitable material for intermolecular hemiacetal bonding with the aldehyde groups of TCNF.

In chapter 1, we developed a biodegradable TCNF/starch membrane with eminent water resistivity by optimizing the concentrations of both polysaccharide derivatives in the TCNF/starch composite. Starch and cellulose are inexpensive biomass resources. However, since neither of them are thermoplastic, there has been no material design to realize a plastic membrane by blending them. When TCNF was mixed with modified starch in an appropriate ratio, we obtained a transparent membrane with excellent in water resistance and mechanical properties; although a membrane consisting only of starch or TCNF respectively collapsed in a short time when immersed in water. The mechanical strength of the composite membrane was greater than that of existing plastic membrane, and the transparency was high enough to replace the existing plastic. The development of polysaccharide membranes using biomass is an innovative material development that contributes to reducing the global environmental impact.

1.2 Experiential section

Materials

Commercially available cellulose powder was supplied by Nacalai Tesque, Japan. Sodium bromide, sodium borohydride and 2,4-dinitrophenylhydrazine (DNPH) were purchased from Sigma Aldrich, Japan. (2,2,6,6-Tetramethylpiperidin-1-yl)oxyl (TEMPO) was supplied by TCI

chemicals, Japan. Sodium hypochlorite was supplied by Nacalai Tesque, Japan. All reagents were laboratory grades. Three types of modified tapioca starch powder, hydroxypropyl starch (HPS, DS: 0.11), acetyl starch (AS, DS: 0.08) and acetyl oxidized starch (AOS, DS: 0.04) were supplied by Nihon Shokuhin Kako Co. Ltd., Japan and used as received. Milli-Q water was used throughout the experiment.

Preparation of cellulose nanofiber (TCNF)

Cellulose nanofiber was prepared by TEMPO-mediated oxidation as reported by Isogai [2]. Briefly, cellulose powder (4.0 g), TEMPO (0.075 g) and NaBr (0.75 g) were added to 300 mL of Mili-Q water and dispersed using magnetic stirring for 1 h at room temperature. The obtained suspension was placed under an automatic titrator (Auto Titrator com -1600, Hiranuma, Japan) to confirm the reaction system maintained at a pH value of 10.5. The total volume of NaClO added was 18 mL. The obtained suspension was treated by centrifugation. After a thorough wash, the cellulose was mechanically treated for 15 min using a blender in order to disperse the cellulose into individual nanofibrils. Concentration of TEMPO-oxidized cellulose nanofibrils (TCNF) in suspension was calculated by weight measurement of before and after lyophilization. The aqueous dispersion of TCNF with a concentration of 0.8% (W/V) was prepared by adding water, and was stored in the refrigerator for further use. Before experiment, suspension was thoroughly stirred to conform the homogeneity.

Preparation of starch solution

Starch powder (5.0 g) was added to 100 mL of Mili-Q water. The suspension was mixed using magnetic stirring at 85 ^{o}C for 1 h to obtain a homogeneous solution. The prepared solution was stored at room temperature for further experiments.

Preparation of TCNF/starch composite membrane

Prepared TCNF dispersion (0.8%, W/V) and starch solution (5%, W/V) were blended together in different weight ratio and stirred until a homogeneous dispersion was obtained. TCNF/starch dispersion was casted in a teflon PFA Petri dish and kept in an oven at 45 ^{o}C for 6 h. Dried membranes were cut into specimens for further experiments.

Preparation of reduced-TCNF (R-TCNF)

$NaBH_4$ was used for the selective reduction of aldehyde moieties on TCNF. 20 g of TCNF was suspended in 40 mL of water and stirred to obtain a homogeneous dispersion. Sodium borohydride (1.0 g) was added to the dispersion with a pH value of about 8, which was adjusted by adding diluted ammonium hydroxide. Subsequently, the slurry was stirred for 24 h and followed by water wash for filtration[9]. Prepared R-TCNF stored in refrigerator for further experiment.

Measurement of aldehyde concentration

Aldehyde group concentration in TCNF and R-TCNF (reduced-TCNF) suspension was measured by the UV-spectrophotometric method using 2,4-dinitrophenylhydrazine (DNPH). 5 mg of DNPH was dissolved in 0.2 mL of concentrated sulphuric acid and stirred to obtain a homogeneous solution. 2 mL of ethanol was added under continuous stirring at room temperature. The mixture was allowed to react for 10 min to achieve homogenization. Final volume was made up to 20 mL by adding water. Prepared DNPH solution was diluted by water into four different concentrations and absorbance at 360 nm was measured for each concentration using a spectrophotometer. A calibration curve for DNPH was plotted in order to formulate standard equation for aldehyde concentration measurement[10,11].

500 µL of TCNF or R-TCNF was added to 5 mL of the prepared DNPH solution, and the mixture was allowed to react for 5 h at room temperature. Unreacted DNPH was collected by centrifugation and absorbance was measured at 360 nm using the spectrophotometer. The amount of aldehyde moieties was calculated as:

$$\text{Aldehyde concentration (µmol/g)} = \frac{\text{Reacted DNPH concentration (µmol)}}{\text{Amount of cellulose in TCNF or R−TCNF (g)}}$$

Characterization

Surface morphology of the dried membranes was observed by SEM (Hitachi SU3500, Japan) at an accelerating voltage of 15 kV and a working distance of 10 mm. Before the SEM examination the surface was sputter coated with platinum-palladium (5 nm thickness) using a vacuum sputtering instrument (Magnetron sputter MSP-1S, Japan). To measure the transparency of the membranes, UV-*vis* spectra of the dried membranes were collected in the wavelength range between 200 nm to 800 nm using a UV spectrometer (Hitachi U-2810, Japan). Data was acquired and analyzed using UV solution 2.0 software. Self-standing dried membranes of thickness 25 µm were used and the air was the blank medium throughout the experiment. Mechanical properties of the membranes were evaluated by a tensile test. Five specimens (20 mm × 5 mm) were cut from each membrane. A micrometer was used to measure their thickness before the test. Measurements were taken at four different positions for each specimen, and the average value was used for the calculation. Tensile test was performed using a universal testing machine (EZ graph, Shimadzu corporation, Japan) with a 100 N load cell and a 0.5 mm/min strain rate. Swelling test was performed in water. Dried membranes specimens (2 cm × 2 cm) were immersed in water. After a fixed time period, swollen samples were gently taken out using tweezers and excess water was

removed with a tissue paper before samples were weighed. Swelling ratio (SR) was calculated as follows:

$$SR\ (\%) = \frac{W_{ss} - W_{ds}}{W_{ds}} * 100$$

where W_{ds} and W_{ss} are weights of the dried and swollen samples, respectively.

The tensile test of swollen membranes was performed using a universal testing machine with a 10 N load cell and 0.5 mm/min strain rate. Three samples were taken from each group for measurement, and the average value of the calculation is reported.

1.3 Results and discussion

Optimization of TCNF/starch composite

Weight ratio of TCNF and modified starch (HPS) in TCNF/starch composite was optimized to cast a membrane possessing adequate dry and wet tensile strength with minimum swelling in water. TCNF and HPS were mixed at different weight ratios as shown in **Table 1-1**. The TCNF/HPS composite was casted into membrane (**Fig. 1-1**) and subsequently characterized by dried and wet membrane tensile test and swelling test, the same as explained above and data are shown in **Table 1-1**.

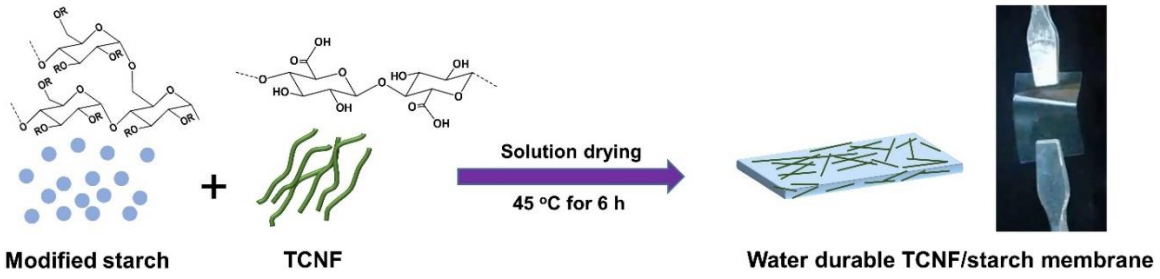

Fig. 1-1. Schematic illustration of TCNF/modified starch membrane prepared by solution casting process.

Dried neat TCNF membrane (N-T) had a tensile modulus of 6.4 GPa. After addition of HPS to TCNF, the obtained dried membrane (S-0.2 and S-0.6) had a higher tensile modulus of 7.6 and 7.3 GPa, respectively. Further increasing the starch concentration in the casted membrane (S-1, S-1.5 and S-6) reduced the tensile modulus to 6.7, 5.7 and 4.8 GPa, respectively (**Fig. 1-2A**).

Table 1-1. Mechanical properties and swelling ratio of TCNF/HPS membranes with different weight ratios of TCNF and HPS.

Group	TCNF : HPS Weight ratio	Tensile modulus of dried membrane (GPa)	Swelling ratio (wt%)	Tensile modulus of wet membrane (MPa)
N –T	1 : 0	6.4 ± 0.2	6720 ± 678	0.05 ± 0.01
S – 0.2	1 : 0.2	7.6 ± 0.3	1337 ± 95	1.61 ± 0.19
S – 0.6	1 : 0.6	7.3 ± 0.1	606 ± 6	7.11 ± 2.17
S – 1	1 : 1	6.7 ± 0.3	698 ± 24	4.07 ± 1.38
S – 1.5	1 : 1.5	5.7 ± 0.4	868 ± 32	1.13 ± 0.20
S – 6	1 : 6	4.8 ± 0.5	924 ± 28	0.21 ± 0.19
N – S	0 : 1	1.6 ± 0.1	Dissolved	Dissolved

These results indicated that the addition of certain starch concentration (S-0.2 and S-0.6) worked as an effective binder between cellulose nanofibers and improved the compatibility of TCNF with each other. Therefore, the dried membrane of S-0.2 had the highest tensile modulus of 7.6 GPa in this experimental conditions.

The swelling properties of each membrane were investigated by immersing them into water. In wet membrane analysis, neat TCNF membrane (N-T) had the highest swelling of ~6500% as shown in **Fig. 1-2C**. Interestingly, water resistance of the membrane had been effectively improved by addition of HPS; swelling ratio of composite membranes decreased to 698%, 868%, 924% and 1337% for S-1, S-1.5, S-6, and S-0.2, respectively. Although neat HPS membrane (N-S) rapidly

dissolved in water. The wet membrane tensile strength and modulus were decreased with increasing swelling ratio, and the highest swollen membrane (neat TCNF) showed minimum wet tensile modulus (0.05 MPa). S-1, S-1.5, S-6, and S-0.2 membranes showed wet tensile modulus of 4.07, 1.13, 0.21, and 1.16 MPa, respectively. Minimum swelling ratio of ~600% was observed in S-0.6, then the highest wet tensile modulus of 7 MPa was observed as shown in **Fig. 1-2B**. These results indicate that there was an optimal combination of TCNF and HPS in terms of water resistance, and that S-0.6 is the best combination.

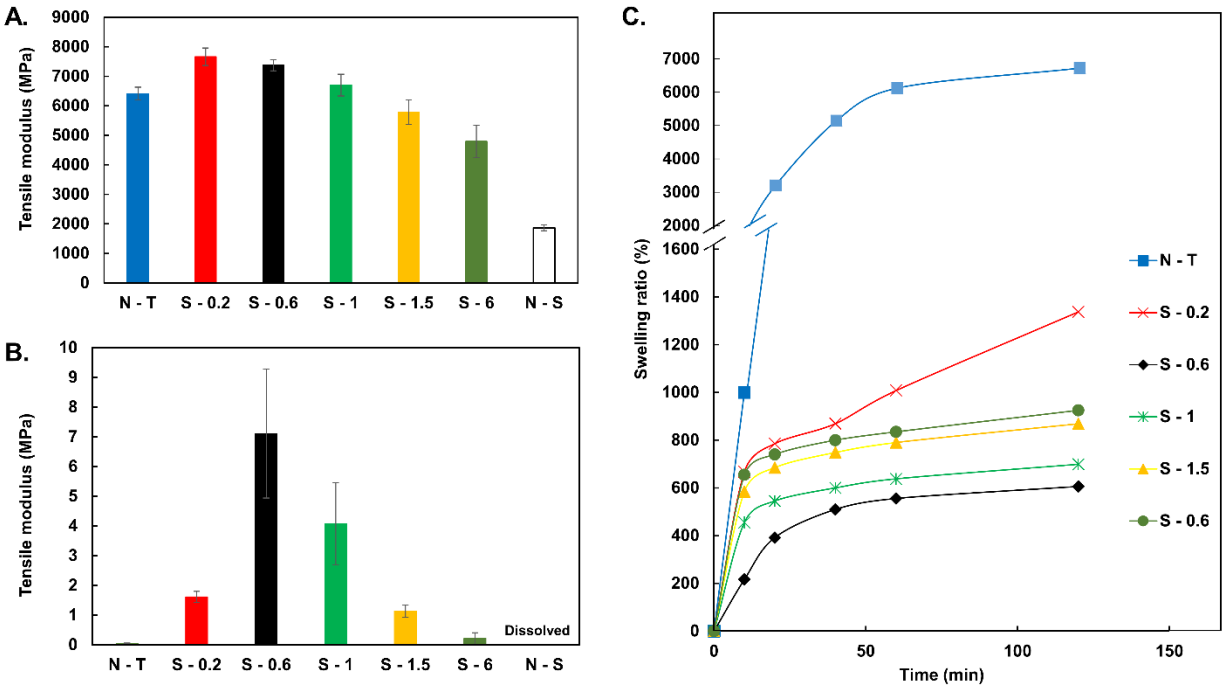

Fig. 1-2. TCNF/HPS membranes with different weight ratios: (A) tensile modulus of dried membranes; (B) tensile modulus of wet membranes; (C) swelling profile of the membranes. Square, cross, circle, triangle, star and diamond symbols indicate N-T, S-0.2, S-6, S-1.5, S-1 and S-0.6, respectively.

During TEMPO oxidation of cellulose, sodium carboxylate and aldehyde moieties were introduced onto the cellulose nanofiber surface. The aldehyde moieties can form hemiacetal bonds by reaction with hydroxyl groups during the drying process of the casting solution. When dried

TCNF membrane is immersed in water, the carboxylate moieties experience strong repulsion among each other, causing intermolecular hemiacetal bonding to lose their strength. Cellulose has a strong hydrophilic nature allowing water molecules to easily bind with the cellulose fiber and partially cross-linked cellulose fiber network creates microgel structure[12]. These microgel structures cause swelling of the dried TCNF membrane (**Fig. 1-3A**). Dried TCNF membrane had a Young's modulus of 6.4 GPa, after immersion in water for 2 h Young's modulus reduced to 0.05 MPa with ~ 6500% swelling of the membrane. However, addition of optimized concentration of starch (S-0.6) formed adequate intermolecular hemiacetal bond, which providing stability and strength to the membrane in water and prevented water molecules to insert into the membrane (**Fig. 1-3B**). Therefore, group S-0.6 membrane has minimum swelling (~600%) and the highest wet tensile modulus (7 MPa).

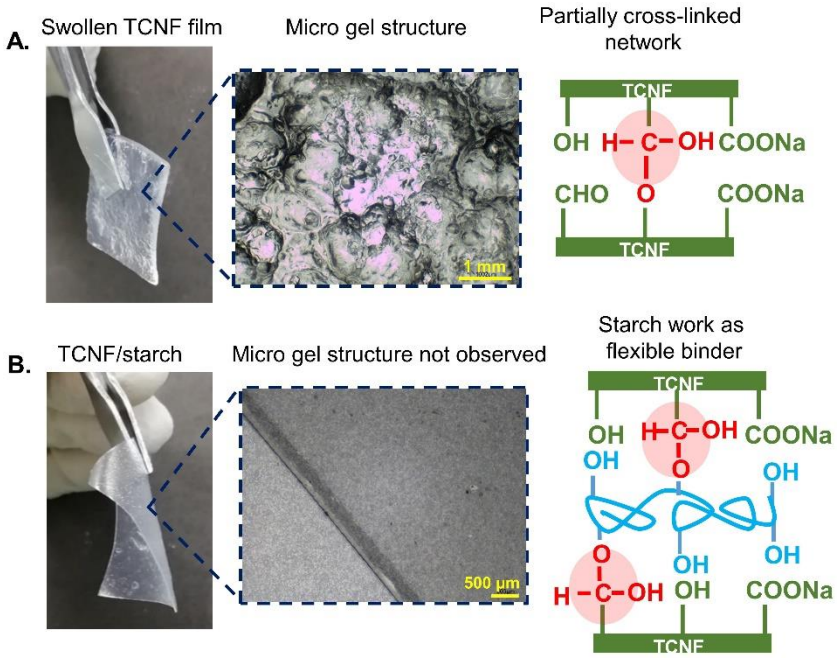

Figure 1-3. (A) Partially cross-linked TCNF film showed microgel structure but (B) addition of starch improved hemiacetal crosslinking and microgel structure not observed.

To confirm the dominating role of the hemiacetal bonding for wet strength and durability of TCNF/HPS membrane, we performed selective reduction of aldehyde moieties in TCNF by sodium borohydride, to form reduced-TCNF (R-TCNF). R-TCNF was mixed with HPS in 1:0.6 ratio, and the mixture was casted into a dried membrane with same conditions as explained above. TCNF/HPS membrane was stable in water but R-TCNF/HPS membrane was disintegrated in water within a few minutes. Aldehyde groups concentration of TCNF was 27 µmol/g, that decreased to 2.2 µmol/g after selective reduction of aldehyde groups on TCNF (**Fig. 1-4**). Therefore, the R-TCNF/HPS membrane disintegrated due to internal carboxylate moieties repulsion (**Fig. 1-5**). This result proved the dominating role of hemiacetal bonding in the water durable TCNF/HPS membrane.

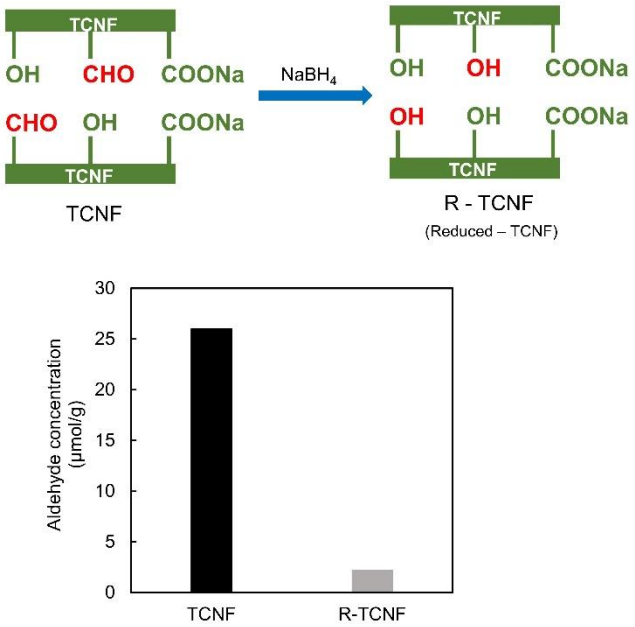

Figure 1-4. Aldehyde moieties concentration before and after $NaBH_4$ reduction

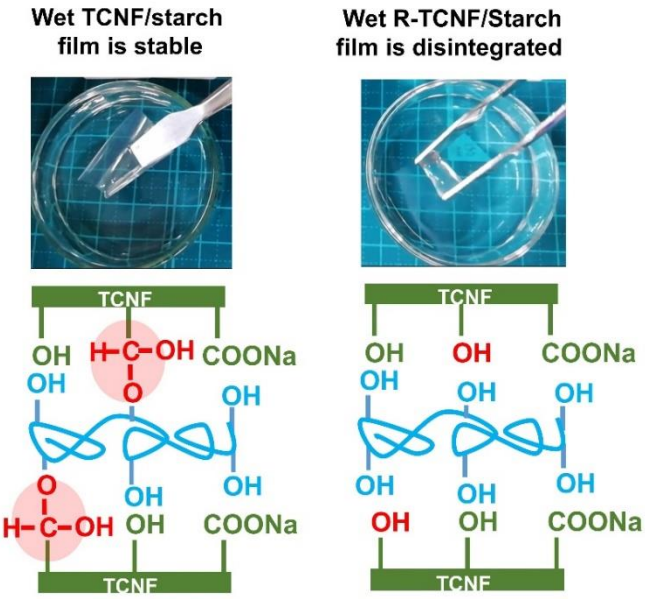

Fig. 1-5. TCNF/HPS and R-TCNF/HPS film stability in water.

Effect of modified starch on TCNF/starch membrane

Three different kinds of modified tapioca starch, hydroxypropyl starch (HPS), acetylated starch (AS) and acetyl oxidized starch (AOS), were used for the preparation of TCNF/starch membrane (TCNF to modified starch ratio is 1:0.6) and composition is shown in **Table 1-2**. Visually, all membranes had high optical transparency, as shown in **Fig. 1-6A**. Transparency of the membrane is an essential property when the membrane is to be used in food packaging. Transmittance of all the dried membranes situated in between 75 to 88 %, for the visual wavelength range from 380 nm to 740 nm as shown in **Fig. 1-6B**. The transmittance at 650 nm was used as the relative value for comparison and data are shown in **Table 1-2**.

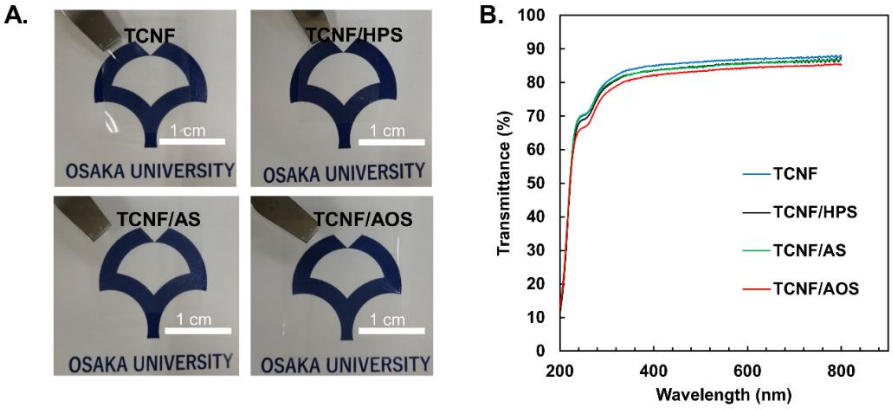

Fig. 1-6. Dried TCNF/starch membranes: (A) optical transparency of the self-standing membranes; (B) UV-spectra of the membranes.

Table 1-2. Tensile properties and optical transparency data of dried membranes casted with different kinds of starch and TCNF blend.

Group	Tensile modulus (GPa)	Tensile strength (MPa)	Strain (%)	Optical Transparency (%) (at 650 nm)
TCNF	6.4 ± 0.2	134 ± 11	3.6 ± 0.2	87
TCNF/HPS[a]	7.3 ± 0.2	125 ± 13	1.7 ± 0.3	86
TCNF/AS[b]	6.7 ± 0.3	105 ± 3	1.6 ± 0.3	85
TCNF/AOS[c]	8.0 ± 0.2	119 ± 22	1.5 ± 0.2	84

[a] Hydroxypropyl starch, [b] acetyl starch, [c] acetyl oxidized starch

Tensile properties of TCNF/starch membranes with varying types of starch were evaluated. Average values of the tensile strength and modulus are summarized in **Table 1-2**. Regardless of the type of starch, tensile modulus of TCNF/starch increased compared to TCNF. As shown in **Fig. 1-7A**, dried TCNF membrane had a smooth surface and a layered cross section. On the other hand, the addition of starch (HPS, AS and AOS) to TCNF caused to disappearance of the layered structure of TCNF (**Fig. 1-7B, C, and D**). These results also indicated that starch worked as a binder to fill between TCNF layers. Moreover, dried TCNF/HPS membrane had smooth surface and starch granules were not observed on the surface and cross-section of the membrane **(Fig. 1-7B**), conforming uniform mixing of TCNF and HPS. On the other hand, many starch granules were observed in the case of TCNF/AOS membrane. Then starch granules may act as fillers for high mechanical strength of AOS composites[13].

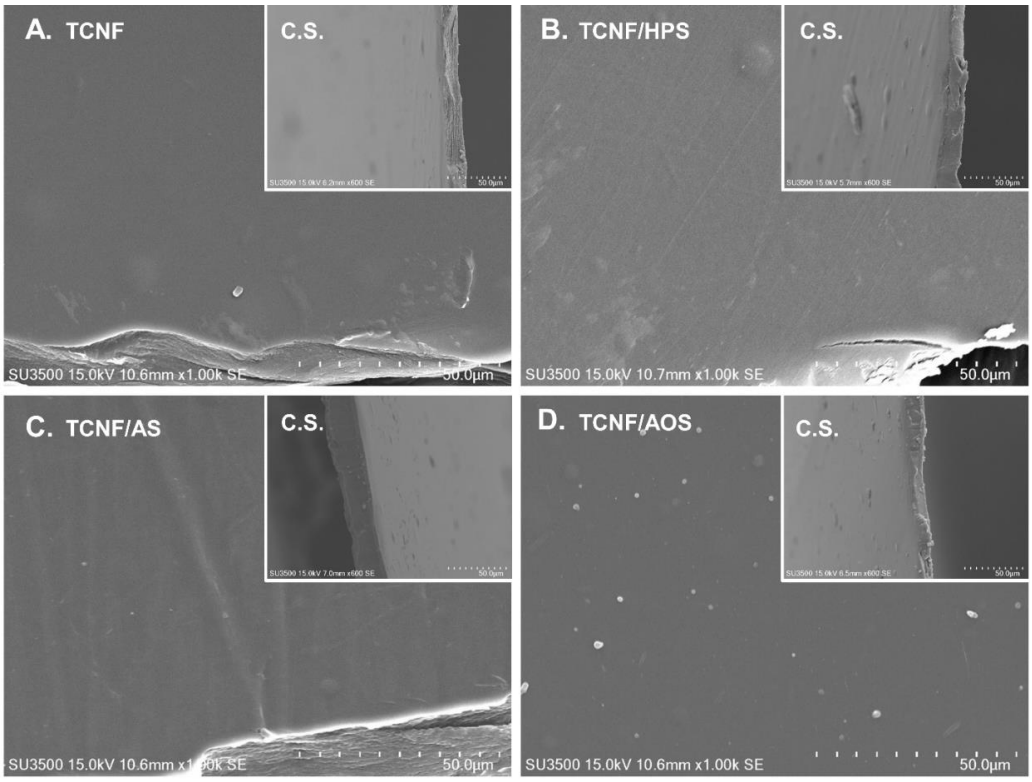

Fig. 1-7. Surface and cross-section morphology of dried membranes: (A) neat TCNF membrane; (B) TCNF/HPS membrane; (C) TCNF/AS membrane; (D) TCNF/AOS membrane.

The water resistance behaviors of these membranes were investigated. **Fig. 1-8A** shows images of swollen membranes after immersion in water for 2 h. All samples were strong enough to be handled with tweezers. The swelling profile of TCNF/starch membranes is shown in **Fig. 1-8B** and the values are summarized in **Table 1-3**. It was found that the swelling ratio decreased even if the starch type was changed. However, the swelling ratio varied depending on the type of starch. TCNF/AOS and TCNF/AS had swelling ratio of 2300% and 1000%, respectively. TCNF/ HPS showed the lowest swelling ratio of 600%.

Wet membranes tensile modulus are shown in **Fig. 1-8C** and the data summarized in **Table 1-3**. The wet membrane tensile properties were higher in all TCNF/starch membranes compared to the neat TCNF membrane. However, the mechanical strength depended on the type of starch. The tensile modulus was found to be 0.06, 2, and 7 MPa for TCNF/AOS, TCNF/AS, and TCNF/HPS membranes, respectively. The water resistance of TCNF/AOS and TCNF/AS were evaluated by changing the composition between TCNF and starch, but the water resistance was remarkably inferior to that of HPS.

Table 1-3. Tensile behaviors and swelling data of the wet TCNF/starch membranes.

Group	Swelling ratio (%) after 2 h	Wet membrane tensile modulus (MPa)	Tensile strength (kPa)
TCNF	6721 ± 678	0.05 ± 0.01	1.5 ± 0.8
TCNF/HPS[a]	606 ± 6	7.12 ± 2.27	300.0 ± 15.0
TCNF/AS[b]	1008 ± 25	2.15 ± 0.18	150.0 ± 8.0
TCNF/AOS[c]	2297 ± 70	0.06 ± 0.01	4.2 ± 1.6

[a] Hydroxypropyl starch, [b] acetyl starch, [c] acetyl oxidized starch

These results can be explained by the chemical structure and microstructure of the modified starch. When comparing AS and AOS, the wet strength of AOS was remarkably low compared to AS, although its mechanical strength in the dry state showed the highest value.

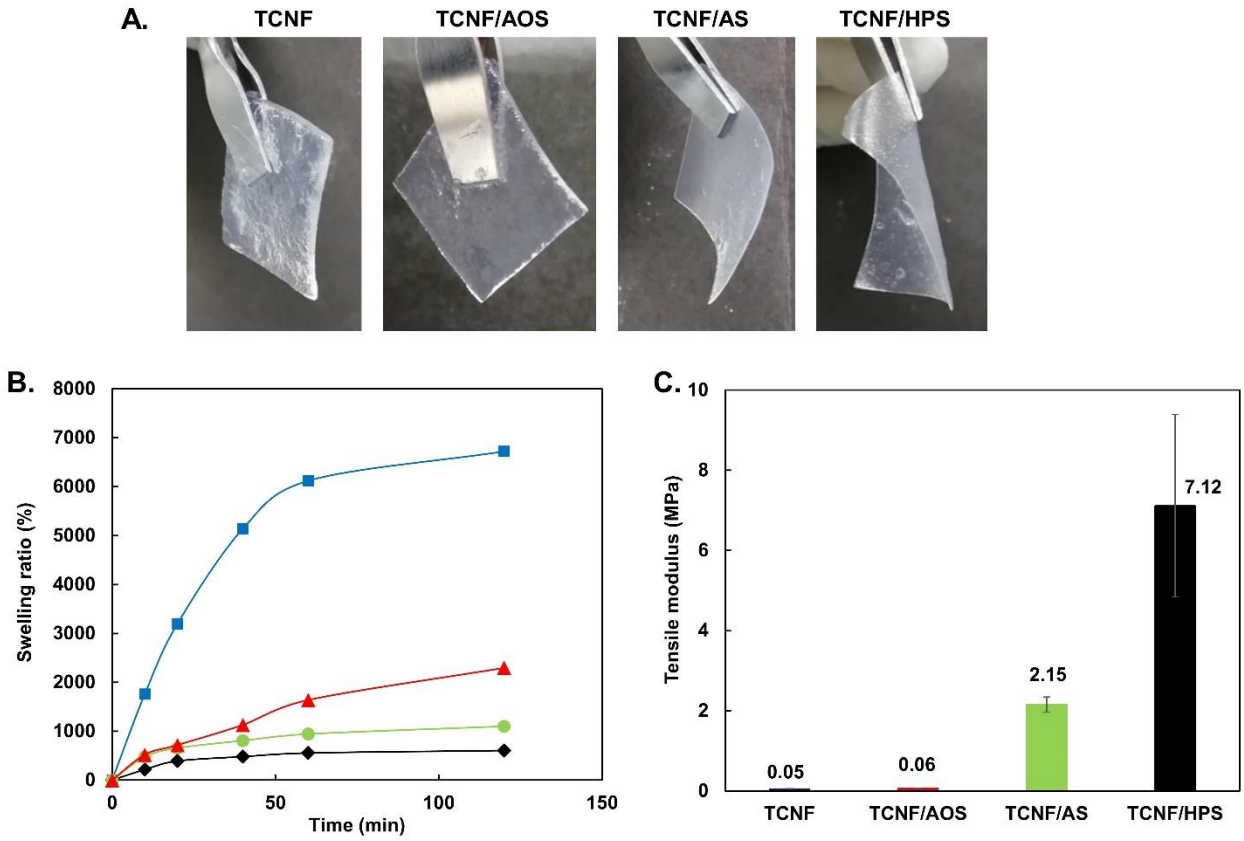

Fig. 1-8. TCNF/starch membranes immersed in water for 2 h: (A) swollen samples after 2 h kept in water; (B) swelling profile of the membranes; (C) tensile modulus of the swollen membranes. In swelling profile graph, square, triangle, circle and diamond represent TCNF, TCNF/AOS, TCNF/AS and TCNF/HPS, respectively.

Due to oxidation of starch, amylose and amylopectin chain depolymerized and amylose content was reduced because of easy to react with oxidant [14,15]. Therefore, AOS has shorter amylose chains, which attributed to diminish strength of intermolecular hemiacetal bonding (**Fig. 1-9**). Moreover, AOS formed granules during the synthesis process. This granule was also observed in SEM observation (**Fig. 1-7D**). It is considered that the mechanical strength in water did not improve

because the effect as a binder was low in case of AOS. In particular, it is clear that the formation of hemiacetal bonds between aldehyde groups of TCNF and hydroxyl groups of starch is important for membranes with a lower swelling ratio. HPS has higher – OH moieties compare to AS and AOS[16]. Additionally, the hydroxypropyl groups are considered to have higher molecular mobility and higher reactivity compared to the hydroxyl groups of starch[17]. Therefore, hemiacetal bonds were effectively formed between HPS and TCNF despite processing from water. These results suggested that the water resistance of the TCNF/starch membrane can be improved by paying attention to the chemical structure of starch and mixing it with TCNF at an appropriate ratio.

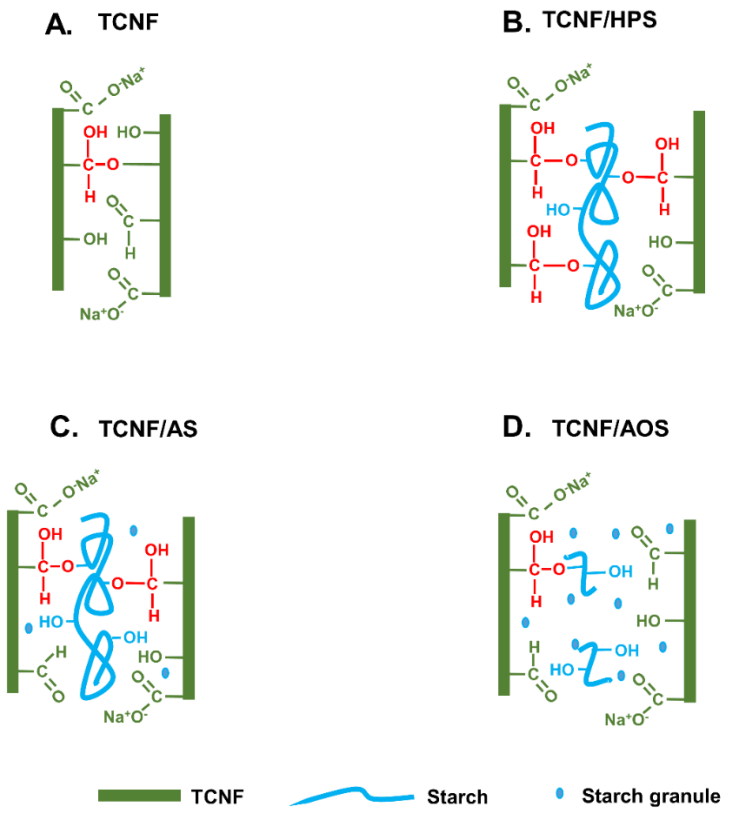

Fig. 1-9. Schematic illustration of intermolecular hemiacetal bonding formation under wet condition: (A) neat TCNF membrane; (B) TCNF/HPS membrane; (C) TCNF/AS membrane; (D) TCNF/AOS membrane.

1.4 Conclusion

In conclusion, we comprehensively studied the effects of mixing three different kinds of starch: (hydroxypropyl starch (HPS), acetyl starch (AS) and acetyl oxidize starch (AOS)) with TEMPO-oxidized cellulose nanofiber (TCNF). TCNF/modified starch membrane casted with 60% cellulose nanofiber/40% starch composite (1**:**0.6 weight ratio) showed minimum swelling with adequate wet strength. The addition of HPS promoted the interaction between TCNF and starch through hemiacetal bonding. Improved wet tensile modulus (7 MPa) and reduced swelling in TCNF/HPS membrane confirm the formation of intermolecular hemiacetal bonding. Recently, the TCNF/HPS membrane has been found to show good biodegradability in marine. Further studies on marine biodegradability of the composite membranes are in progress. We believe that the TCNF reinforced HPS membrane opens the research for the next generation renewable, biodegradable, water durable high performance - green packaging membrane.

1.5 References

(1) Isogai, A. *Proc. Jpn. Acad. Ser. B. Phys. Biol. Sci.* **2018**, *94* (4), 161–179.

(2) Isogai, A.; Saito, T.; Fukuzumi, H. *Nanoscale* **2011**, *3* (1), 71–85.

(3) Isogai, A.; Hänninen, T.; Fujisawa, S.; Saito, T. *Prog. Polym. Sci.* **2018**, *86*, 122–148.

(4) Maloney, T. C. *Holzforschung* **2015**, *69* (2), 207–213.

(5) T. S.; Isogai*. *Ind. Eng. Chem. Res.* **2007**, 46, 3, 773–780

(6) Saito, T.; Isogai, A. *Colloids Surfaces A Physicochem. Eng. Asp.* **2006**, *289* (1–3), 219–225.

(7) Sun, B.; Hou, Q.; Liu, Z.; Ni, Y. *Cellulose* **2015**, *22* (2), 1135–1146.

(8) Lu, D. R.; Xiao, C. M.; Xu, S. J. *Express Polym. Lett.* **2009**, *3* (6), 366–375.

(9) Potthast, A.; Schiehser, S.; Rosenau, T.; Kostic, M. In *Holzforschung*; Walter de Gruyter, **2009**; Vol. 63, pp 12–17.

(10) Ruekberg, B.; Rossoni, E. *J. Chem. Educ.* **2005**, *82* (9), 1310.

(11) Tummalapalli, M.; Gupta, B. *J. Carbohydr. Chem.* **2015**, *34* (6), 338–348.

(12) Torstensen, J. Ø.; Liu, M.; Jin, S.-A.; Deng, L.; Hawari, A. I.; Syverud, K.; Spontak, R. J.; Gregersen, Ø. W. *Biomacromolecules* **2018**, *19* (3), 1016–1025.

(13) Le Corre, D.; Angellier-Coussy, H. *React. Funct. Polym.* **2014**, *85*, 97–120.

(14) Fonseca, L. M.; Gonçalves, J. R.; El Halal, S. L. M.; Pinto, V. Z.; Dias, A. R. G.; Jacques, A. C.; Zavareze, E. da R. *LWT - Food Sci. Technol.* **2015**, *60* (2), 714–720.

(15) Sandhu, K. S.; Kaur, M.; Singh, N.; Lim, S.-T. *LWT - Food Sci. Technol.* **2008**, *41* (6), 1000–1010.

(16) Fu, Z.; Zhang, L.; Ren, M.-H.; BeMiller, J. N. *Starch - Stärke* **2019**, *71* (1–2), 1800167.

(17) Yoshioka, S.; Aso, Y. *J. Pharm. Sci.* **2007**, *96* (5), 960–981.

Chapter 2

Synergistic effect of hemiacetal crosslinking and crystallinity on wet strength of cellulose nanofiber reinforced starch film

2.1 Introduction

Starch is a biocompatible, biodegradable, renewable, and abundant polysaccharide[1]. Starch is formed by two types of polymers: amylose and amylopectin. Amylose is essentially a linear chain with limited branching points. Amylopectin (starch constitution, 70-85%) consists of linear chains of glucose units interspersed by highly branching small glucose chains every 10 nm along the molecular axis[2]. However, packaging films that are prepared from starch pastes have low water resistance and dissolve within a few minutes.

Previously, starch incorporates with many inorganic fillers as silica, $CaCO_3$, alumina, etc., to improve water durability[3–5]. However, the optical, mechanical properties and recyclability of such films are detrimentally affected. Aldehydes might be the most frequently used chemicals for starch crosslinking due to their high reaction efficiency to form hemiacetal/acetal crosslinking. Glutaraldehyde and formaldehyde are examples of aldehydes that are most widely used in crosslinking starch-based composite to enhanced water durability[6–8]. However, hazards and toxicity restrict their application on a large scale. Aldehyde moieties introduced to polysaccharides to prepare environmental friendly cross linkers. Starch film crosslinked by oxidized sucrose (di-aldehyde sucrose), di-aldehyde starch, and di-aldehyde cellulose (~100% oxidized, amorphous) had water stability due to hemiacetal crosslinking[9–12], however, film possess poor wet strength owing to highly amorphous.

Crystallinity also influence starch film water durability and wet strength. Addition of cellulose nanocrystal, or micro fibrillated cellulose improved crystallinity of starch/cellulose film, and enhanced the film water durability[13]. TEMPO oxidation of cellulose resultant highly fibrillated TCNF with a high aspect ratio (4-20 nm) and crystallinity (~74%) that possess some aldehyde moieties (~27 mmol/g) as intermediate structures on the surface[14–16]. A composite film of starch with TEMPO-oxidized cellulose nanofibers (TCNF) exhibited high water stability and wet strength[17]. Therefore, hemiacetal crosslinking and crystallinity both have a key role in improving wet strength.

The crystallinity of starch depends on the reassociation of amylose and amylopectin in the starch paste[18,19]. Moreover, the reassociation process directly depends on starch paste storage time and conditions. Thus, starch crystallinity can be changed by optimized starch paste storage time in control conditions. Also, Starch modification as hydroxypropylation, acetylation, oxidation, etc., not only changes the hemiacetal crosslinking due to modified moieties reactivity, and changes crystallinity to slow down the reassociation process in the starch paste[20–22]. Therefore, the starch paste storage time should be considered for optimizing the synergistic effect of hemiacetal crosslinking and crystallinity on TCNF-modified starch films.

In chapter 2, we optimized the storage time of the starch paste for achieving the synergistic effect of hemiacetal crosslinking and crystallinity on TCNF/starch films. Three types of starch (different physiochemical structure and reactivity to form hemiacetal crosslinking), namely native tapioca starch (NTS), hydroxypropyl starch (HPS), and di-aldehyde starch (Di-aldS) pastes, were blended with TCNF after storing the starch pastes for different numbers of days. Further, several characterization tests (as rheology, mechanical test, optical analysis, swelling, and wet tensile test) were performed to optimize the paste storage time to get the most suitable crystalline arrangement

and crosslinking for higher film properties. In addition, the most acceptable TCNF/starch composite was demonstrated for different applications. Thus, optimizing the TCNF/starch film properties by controlling the starch paste storage time is an innovative, environment-friendly, and adaptable industrial method.

2.2 Experimental section

Materials

Commercially available cellulose powder and sodium hypochlorite were supplied by Nacalai Tesque, Japan. Sodium bromide (NaBr) was purchased from Sigma-Aldrich, Japan. (2,2,6,6-Tetramethylpiperidin-1-yl)oxyl (TEMPO) was supplied by TCI Chemicals, Japan. All reagents were laboratory-grade. NTS (17-20% amylose and 83-80% amylopectin), HPS (molar substitution, 0.1), and Di-aldS (molar fraction, 5.4) powders were supplied by Nihon Shokuhin Kako Co. Ltd., Japan and used as received. Milli-Q water was used throughout the experiments. TCNF was prepared same as explain in chapter 1.

Preparation of the starch paste

NTS, HPS, and Di-aldS powders (5.0 g) were added to 100 mL of Milli-Q water. The suspensions were mixed using magnetic stirring and gelatinized at 90 $^{\circ}$C for 1 h, to obtain homogeneous starch pastes. The prepared starch pastes were immediately used for film preparation (represented as day 0). In each case, some of the starch paste was stored at close container (~22 $^{\circ}$C, ~25% RH) for 1,3,5,7, and 10 days for amylose and amylopectin reassociation. The reassociated starch pastes were shaken thoroughly before being used for film preparation.

Preparation of films

The prepared TCNF suspension (~1% w/v) and starch pastes (5% w/v) were blended at different days of reassociation, and stirred until homogeneous dispersions were obtained. The TCNF/starch dispersions were cast in polypropylene petri dishes, and were kept in an oven at 45 °C for 6 h. The prepared dried films were cut into specimens and stored in close container (~22 °C, ~25% RH), and were referred to as "TCNF/starch_day" in the experiments.

Marine microbial degradation test

Prepared TCNF and TCNF/HPS films were cut into 15 mm square using scissors and used as the degradation test sample. For the marine microbial degradation test, films were placed on whalebone, which was kept at 4 °C in a tank simulating the marine environment. The whalebone sample was collected from Nojima tidal put inside a container full fill with artificial seawater simulating intertidal zone. Whalebone provided support and required nutrition to grow marine microbes. The films were kept in plastic cell strainers (Falcon, 40μm nylon mesh) and covered with glass slides to prevent floating. The samples were incubated for 4 weeks.

After completing the incubation period, the films were immediately fixed with glutaraldehyde solution and dried using a water freeze-drying apparatus. The dried samples were followed by surface morphology analysis using SEM imaging.

Characterization

A stress-controlled rheometer (Haake Rheo Stress 6000, Thermo Scientific) was used to examine the rheological behavior of the obtained TCNF/starch suspensions. All of the measurements were conducted with an aluminum cone-plate geometry (diameter, 40 mm; angle, 2°). The strain amplitude value selected was 0.01, which was in the linear viscoelastic region for all samples. Frequency sweeps were performed from 0.1 to 10 rad/s. A temperature controller

(Haake UTM controller, Thermo Scientific) was used to maintain temperature (25 °C) during the measurements. X-ray scattering measurements of the dried films were performed using a SmartLab X-ray diffractometer (Rigaku Corporation, Japan) equipped with a copper tube operating at 40 kV and 200 mA. Diffractograms were obtained by scanning from 5° to 40° (2θ) at a rate of 5°/min, step size of 0.02°, and scatter slit width of 1°. Data were acquired and analyzed using SmartLab Studio software. A haze meter (Haze meter NDH 4000, Nippon Denshoku Kogyo Co. Ltd.) was used for measuring the haze of the films. Self-standing dried films (thickness, 25 µm) were used, and the air was the blank medium throughout the experiment. Dried and wet film mechanical test and swelling analysis performed same as explain in chapter 1.

2.3 Results and Discussion

Effect of the starch paste storage time on dried films

To analyze the effect of the native starch paste storage time, we prepared an NTS paste and stored it at close container (~22 °C, ~25% RH) for 0, 1, 3, 7, and 10 days, respectively. On each day of interest, the prepared starch paste was mixed with the prepared TCNF dispersion (1:0.6, TCNF**:** starch). Further, the TCNF/NTS suspensions were converted into films using the solvent casting method; the prepared films were referred to as "TCNF/NTS_ day" in the experiments.

Self-standing TCNF/NTS films were prepared using the starch pastes stored for different numbers of days, as shown in **Fig. 2-1**. TCNF/NTS_0 and TCNF/NTS_3 had 15% and 17% haze, respectively. However, the films cast with longer-stored starch paste samples exhibited higher haze values (38% and 47% for TCNF/NTS_7 and TCNF/NTS_10, respectively). The dried films strain energy density and crystallinity of the prepared TCNF/NTS films are shown in **Fig. 2-2,** and the data are summarized in **Table 2-1**. TCNF/NTS_0 had a strain energy density of 972 kJ/m^3, which

increased to 1042 kJ/m^3 for TCNF/NTS_1. However, the strain energy density then monotonically decreased to 924, 730, and 518 kJ/m^3 for TCNF/NTS_3, TCNF/NTS_7, and TCNF/NTS_10 films.

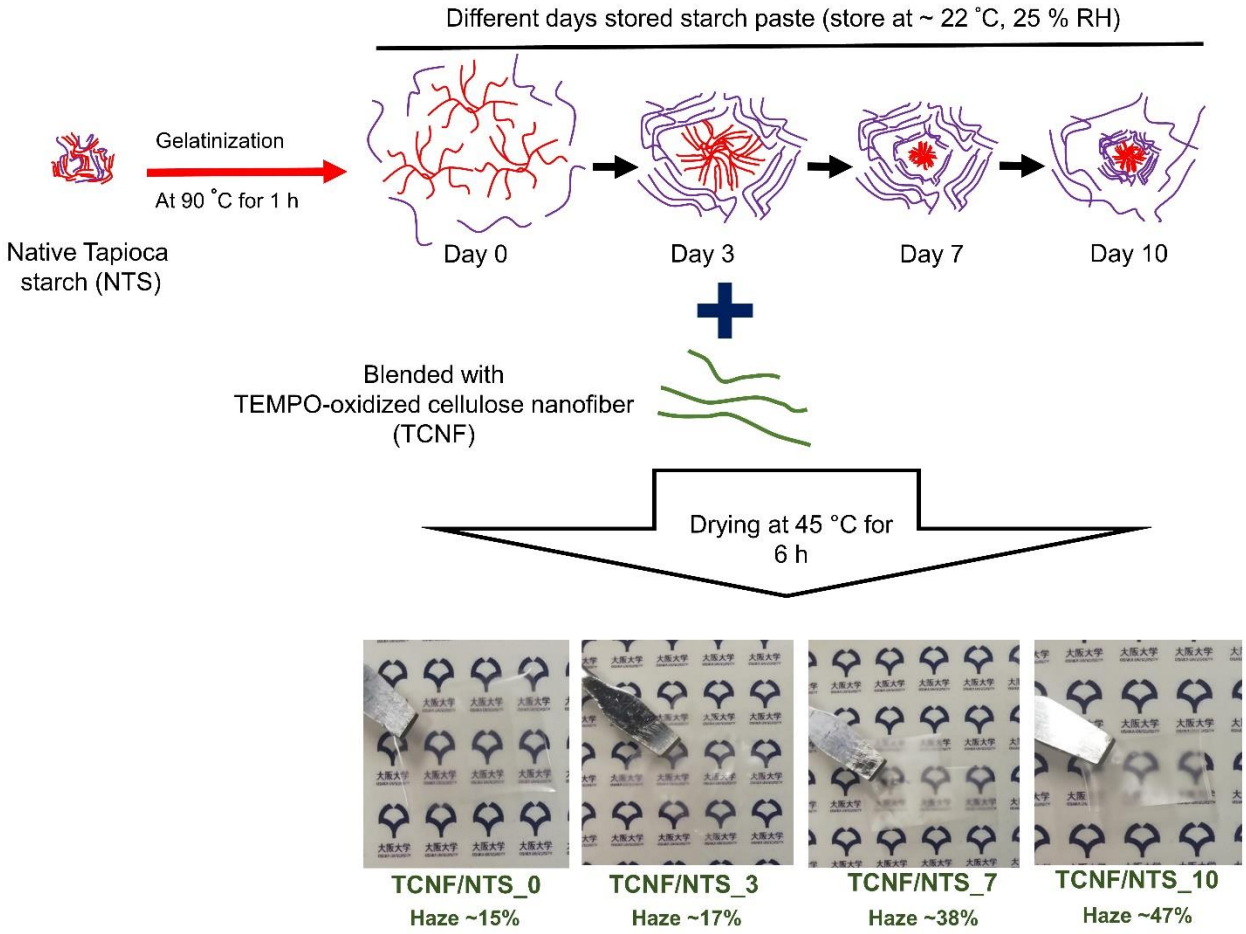

Figure 2-1. Preparation of TCNF/NTS films from TCNF and NTS paste samples with different storage times.

During the initial storage period, amylose and amylopectin chains were well-dispersed in the starch paste. The interaction between the starch and TCNF reduced mobility and hence improved rigidity[23]. Therefore, the film become tough and strain energy density increased significantly for the TCNF/NTS_1 film. However, for longer storage times, a homogeneous starch paste is known

to convert into a non-homogeneous dispersion of amylose, amylopectin with reassociated starch granules[20], a phenomenon known as starch retrogradation.

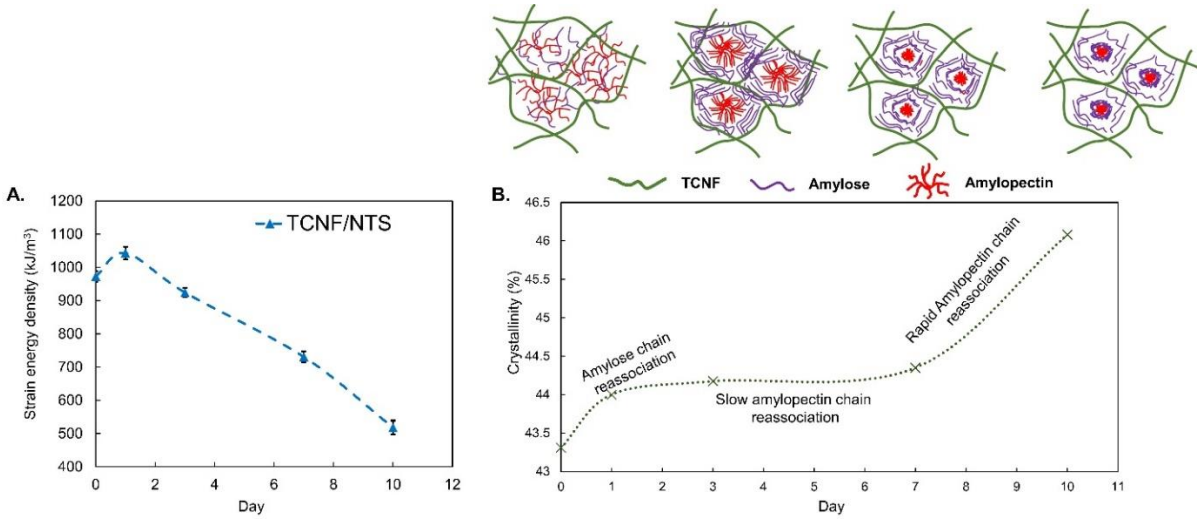

Figure 2-2. (A) Strain energy density and (B) crystallinity of the TCNF/NTS films prepared with different-storage-time NTS paste samples.

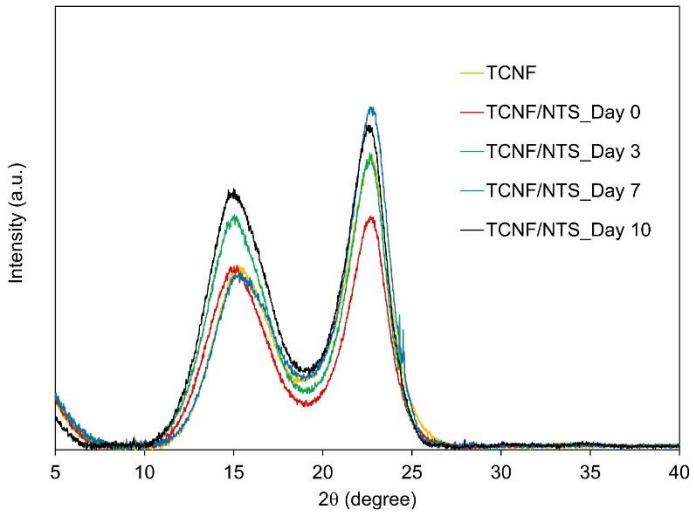

Figure 2-3. XRD of TCNF/NTS films prepared using different storage-duration NTS pastes.

These larger starch granules increased the haze of the casted film (TCNF/NTS_7). This retrogradation is an ongoing process, and the size of the reassociated starch granules increased with increasing the storage duration. Therefore, the haze value rapidly increased for

TCNF/NTS_10. In addition, the excess size of the reassociated granules diminished the interaction between the starch and TCNF[4]. Therefore, the film become brittle and the strain energy density started to decrease.

Further, the reassociation of the starch polymer chains was confirmed by measuring the crystallinity of the TCNF/NTS films. The crystallinity results for the TCNF/NTS films prepared on the different days of the NTS paste storage are shown in Fig. 2B, and the corresponding XRD curves are shown in Fig. 2-3**.** The TCNF/NTS_0 film exhibited randomly oriented amylose and amylopectin molecules, and its crystallinity was 43.4%. The starch paste crystallinity increased owing to reassociation of amylose and amylopectin, with increasing the storage time[18]. The crystallinity peaks for starch and cellulose were observed for 2θ values ranging from 10 to 30, in the XRD analysis. Therefore, the overall crystallinity of the TCNF/NTS films increased, due to the superimposition of the starch crystallinity peaks on the cellulose peaks, because the crystallinity of the TCNF component was the same throughout the experiments.

The TCNF/NTS_1 film exhibited enhanced crystallinity of 43.9%, owing to the rapid reassociation of the amylose chains. Because the amylopectin chain reassociation is a slow process[24], a slight change in crystallinity was observed for NTS_3 and NTS_7 cast films. After a long storage time, rapid reassociation in amylopectin occurred. Therefore, the crystallinity of the TCNF/NTS_10 film increased dramatically (45.8%). Thus, dried TCNF/NTS films

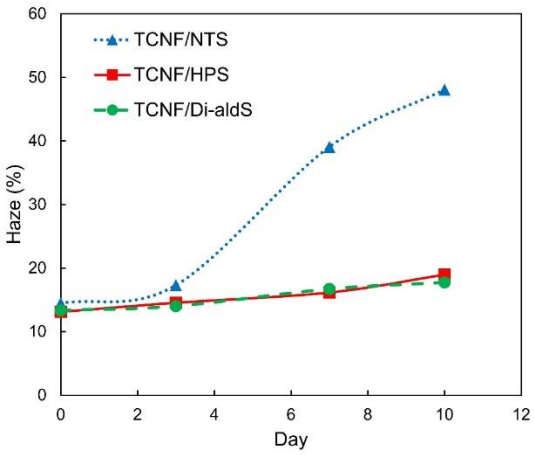

Figure 2-4. Dependence of haze on the storage duration, for TCNF/NTS, TCNF/HPS, and TCNF/Di-aldS films prepared with different storage-duration starch pastes.

exhibited very significant dependence of their optical and mechanical properties on the storage time (starch paste crystallinity) of the NTS paste.

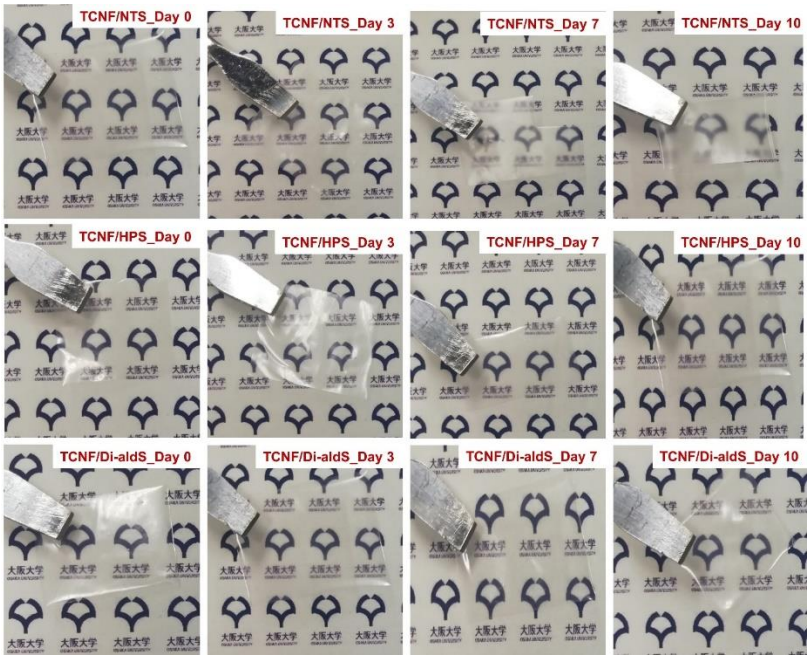

Figure 2-5. Optical images of self-standing TCNF/NTS, TCNF/HPS, and TCNF/Di-aldS films prepared with different storage-duration starch pastes.

To analyze the storage-time effect of modified starch pastes, HPS and Di-aldS were used for preparing TCNF-modified starch films. We prepared HPS and Di-aldS pastes and stored them at the same time and conditions as explained above. The stored modified starch pastes were blended with TCNF (1:0.6, TCNF**:**starch) at respective days, and were referred to as "TCNF/modified starch_Day" in the experiments. TCNF/NTS, TCNF/HPS, and TCNF/Di-aldS films, prepared on different days of the starch pastes storage, are shown in **Fig. 2-4, 5**.

Tensile strength and strain energy density of dried TCNF/modified starch films prepared on different days of the modified starch pastes storage are shown in **Fig. 2-6,** and the corresponding data are summarized in **Table. 2-1**. TCNF/HPS_0 and TCNF/Di-aldS_0 had tensile strength ~91

and ~95 MPa, and strain energy density of 969 and 926 kJ/m^3, respectively. The TCNF-modified starch films exhibited the same behavior as the TCNF/NTS films. Amylose and amylopectin reassociation enhanced the interaction between the starches and TCNF, and the tensile strength and strain energy density of the TCNF/HPS_3 and TCNF/Di-aldS_1 films increased to 110 MPa, 1080 kJ/m^3 and 115 MPa, 992 kJ/m^3, respectively. However, excess storage caused the formation of starch granules.

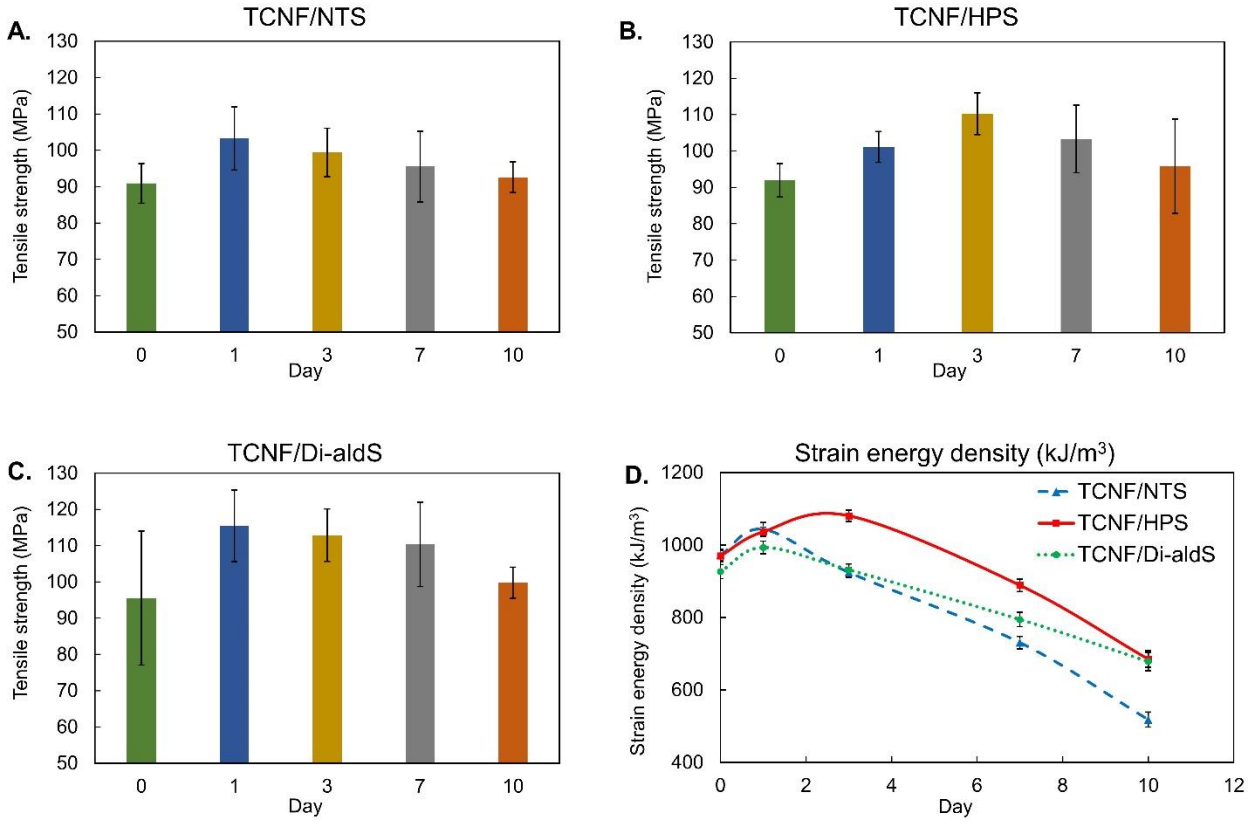

Figure 2-6. Dried film tensile strength of (A) TCNF/NTS (B) TCNF/HPS (C) TCNF/Di-aldS films and (D) comparative analysis of strain energy density of the films prepared with different day stored starch paste.

Therefore, the interaction between starch and TCNF fibers was reduced, and the film become brittle. The tensile strength and strain energy density decreased to ~95 MPa, 685 kJ/m^3 and ~99 MPa, 678 kJ/m^3, for TCNF/HPS_10 and TCNF/Di-aldS_10, respectively. Starch modification

reduced the reassociation rates of amylose and amylopectin owing to modified moieties[25]. Therefore, the reassociation process was slow for the HPS paste, and the TCNF/HPS films did not exhibit much variation in the haze value, even after 10 days of storage (**Fig. 2-4**). Moreover, the TCNF/HPS_3 film showed the highest strain energy density (1080 kJ/m^3), owing to the stronger polymer chain interactions of the hydroxypropyl moieties.

Table 2-1. Mechanical behavior of dried TCNF-modified starch films prepared on different days of the starch paste storage.

Starch paste storage time	TCNF/NTS			TCNF/HPS			TCNF/Di-aldS		
	Strength (MPa)	**Strain (%)**	**Strain energy density (kJ/m^3)**	**Strength (MPa)**	**Strain (%)**	**Strain energy density (kJ/m^3)**	**Strength (MPa)**	**Strain (%)**	**Strain energy density (kJ/m^3)**
Day 0	90.89±5.47	2.14±0.26	972±15	91.93±4.61	2.11±0.13	969±15	95.52±18.45	1.94±0.10	926±19
Day 1	103.26±8.70	2.02±0.20	1042±18	101.09±4.23	2.05±0.14	1036±12	115.45±9.91	1.72±0.15	992±17
Day 3	99.39±6.71	1.86±0.32	924±13	110.25±5.72	1.96±0.20	1080±15	112.89±7.21	1.65±0.17	931±16
Day 7	95.52±9.75	1.53±0.35	730±17	103.34±9.31	1.72±0.16	888±17	110.34±11.61	1.44±0.20	794±19
Day 10	92.56±4.19	1.12±0.51	518±20	95.81±12.93	1.43±0.35	685±22	99.8±4.28	1.36±0.25	678±25

NTS = native tapioca starch, HPS = hydroxypropyl starch, Di-aldS = di-aldehyde starch

Dried TCNF/Di-aldS films exhibited the highest tensile strength and lesser strain energy density, representing brittle behavior of the films. In addition, depolymerized starch chains do not favor reassociation process[26]. Therefore, the TCNF/Di-aldS films did not exhibit any significant haze value variations after 10 days of storage. These results suggest that the films prepared with modified starch pastes exhibited the same variation in their mechanical properties as their corresponding native starch paste, but rate of variation in properties was less due to slow reassociation process. Moreover, the optical properties of TCNF/modified starch films showed

less change. Thus, changes in crystallinity of starch paste drastically affected mechanical properties of TCNF/modified starch film.

Effect of the starch paste storage time on wet films

The prepared TCNF/modified starch films were kept in water for 2 h, for comparative analysis of the modified starch pastes storage duration on swelling and wet strength. The swelling ratio (SR), wet tensile strength, and wet strain energy density of the studied TCNF/starch films are shown in **Fig. 2-7,** and the corresponding data are summarized in **Table 2-2**.

For the TCNF/NTS_0 film, the SR was ~333%, the wet tensile strength was 0.70 MPa, and the wet strain energy density was 55.13 kJ/m^3. However, for the TCNF/NTS_10 film, the SR was ~1700%, while its wet tensile strength of ~0.09 MPa was the lowest, and its wet strain energy density was ~7.87 kJ/m^3. The TCNF/NTS_1 film exhibited the lowest SR of ~273%, with a higher wet tensile strength of ~1.04 MPa, while its wet strain energy density was 123.82 kJ/m^3.

The same behavior was observed for the TCNF/HPS and TCNF/Di-aldS films. The TCNF/Di-aldS_1 and TCNF/Di-aldS_10 films exhibited the SRs of ~366% and ~725%, respectively, and their wet tensile strengths were 0.81 MPa and 0.47 MPa, respectively. The TCNF/HPS_1 and TCNF/HPS_10 films exhibited the SRs of ~302% and ~637%, respectively, and their wet tensile strengths were 0.89 MPa and 0.66 MPa, respectively. The highest wet strength of ~1.17 MPa, and the strain energy density of 133.3 kJ/m^3, were obtained for the TCNF/HPS_3 film. Thus, the water-resistance behavior of TCNF/starch films increased during the initial starch storage period. However, the SR increased, and the wet strength decreased with longer storage duration.

TCNF have anionic carboxylate moieties that generate strong electrostatic repulsion, disturbing the fibers arrangement in wet conditions[27]; thus, pristine TCNF films exhibited the SR

of ~6000%. However, the composite of starch_day 0 with TCNF worked as an effective binder by forming hemiacetal crosslinking between the hydroxyl moieties of starch and the aldehyde moieties of TCNF, thus avoiding water penetration in the resulting TCNF/starch film. Therefore, TCNF/NTS_0, TCNF/HPS_0, and TCNF/Di-aldS_0 films exhibited lower SRs of ~333%, ~302%, and ~366%, respectively. Hydroxypropyl moieties had higher reactivity for forming hemiacetal crosslinking; consequently, TCNF/HPS_0 exhibited less swelling. Because Di-aldS contains depolymerized starch chains that diminish the hemiacetal crosslinking strength[28], TCNF/Di-aldS_0 exhibited higher swelling.

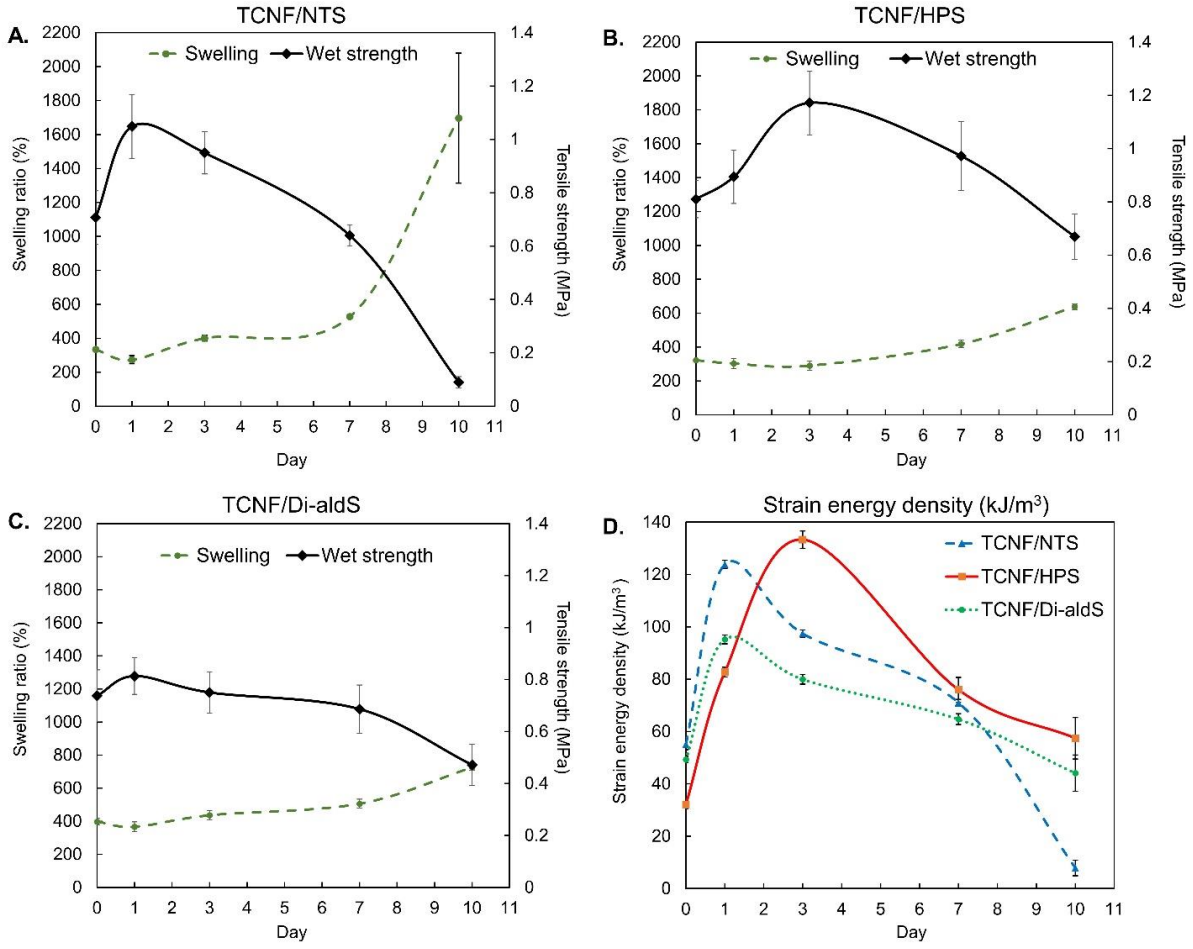

Figure 2-7. Swelling ratio and wet tensile strength dependence on the starch paste storage duration, for (A) TCNF/NTS, (B) TCNF/HPS, and (C) TCNF/Di-aldS films. (D) Strain energy density of swollen TCNF-modified starch films, vs. the storage duration, for different pastes.

Table 2-2. Swelling ratio, wet tensile strength, and strain energy density of TCNF-modified starch films prepared using different storage-duration starch pastes.

Starch retrogradation	TCNF/NTS			TCNF/HPS			TCNF/Di-aldS		
	Swelling (%)	**Wet strength (MPa)**	**Strain energy density (kJ/m^3)**	**Swelling (%)**	**Wet strength (MPa)**	**Strain energy density (kJ/m^3)**	**Swelling (%)**	**Wet strength (MPa)**	**Strain energy density (kJ/m^3)**
Day 0	333.46±11.08	0.70±0.10	55.13±2.02	322.13±11.19	0.81±0.07	32.09±1.67	397.58±20.43	0.73±0.11	49.30±1.17
Day 1	273.17±23.58	1.04±0.12	123.82±1.58	302.86±29.72	0.89±0.10	82.71±1.89	366.04±30.41	0.81±0.07	95.19±1.65
Day 3	400.08±16.69	0.95±0.08	97.42±1.41	290.29±25.83	1.17±0.12	133.32±3.29	435.96±28.64	0.75±0.080	79.95±1.56
Day 7	526.99±9.79	0.64±0.04	71.01±1.22	417.72±21.94	0.97±0.13	75.94±4.80	505.87±26.87	0.68±0.093	64.71±2.08
Day 10	1696.77±383.01	0.09±0.021	7.87±2.97	637.75±17.75	0.66±0.086	57.44±7.94	725.43±18.78	0.47±0.079	44.10±6.94

NTS = native tapioca starch, HPS = hydroxypropyl starch, Di-aldS = di-aldehyde starch

Gelatinization destroys the crystalline structure of starches; consequently, day-zero starch pastes are amorphous. During the starch paste storage, amylose and amylopectin reassociate and form crystalline network structures that enhance water durability. Thus, the blending of crystalline starches with TCNF improved the water durability and strength of the TCNF/starch films owing to the synergistic effect of hemiacetal crosslinking and starch crystallinity. Therefore, TCNF/NTS_1, TCNF/HPS_3, and TCNF/Di-aldS_1 exhibited less swelling. We observed the highest wet strength and strain energy density for the TCNF/HPS_3 film, owing to its higher hemiacetal crosslinking density.

Longer-duration storage promotes the formation of large-size starch granules[29]. The starch crystallinity increased, but its crosslinking density decreased due to the formation of granules. In addition, starch granules disturbed the fiber packaging of the films. Therefore, TCNF/NTS_10, TCNF/HPS_10, and TCNF/Di-aldS_10 exhibited higher swelling. Rapid

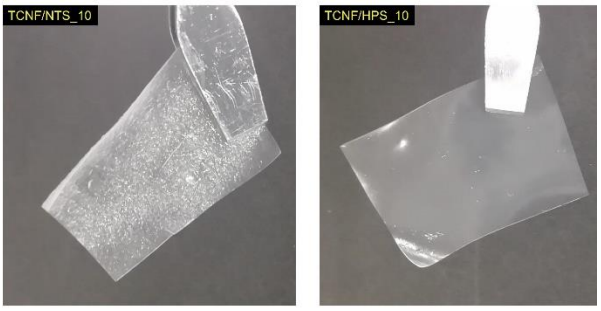

Figure 2-8. Swollen films of TCNF/NTS_10 and TCNF/HPS_10.

reassociation in native starch induced more extensive granule formation; thus, TCNF/NTS_10 exhibited the highest swelling (~1700%) and the lowest wet strength (**Fig. 2-8**).

Changes in polymer packaging with the starch paste storage time in TCNF/starch suspensions were confirmed by rheological analysis. Variations in the storage moduli (G') and loss moduli (G'') of the prepared TCNF/starch suspensions were investigated for frequencies ranging from 0.1 to 10 rad/s, and the results are shown in **Fig. 2-9**. The values of G' and G" at the frequency of 1 rad/s were used as the relative values for comparison, and the results are summarized in **Table 2-3**.

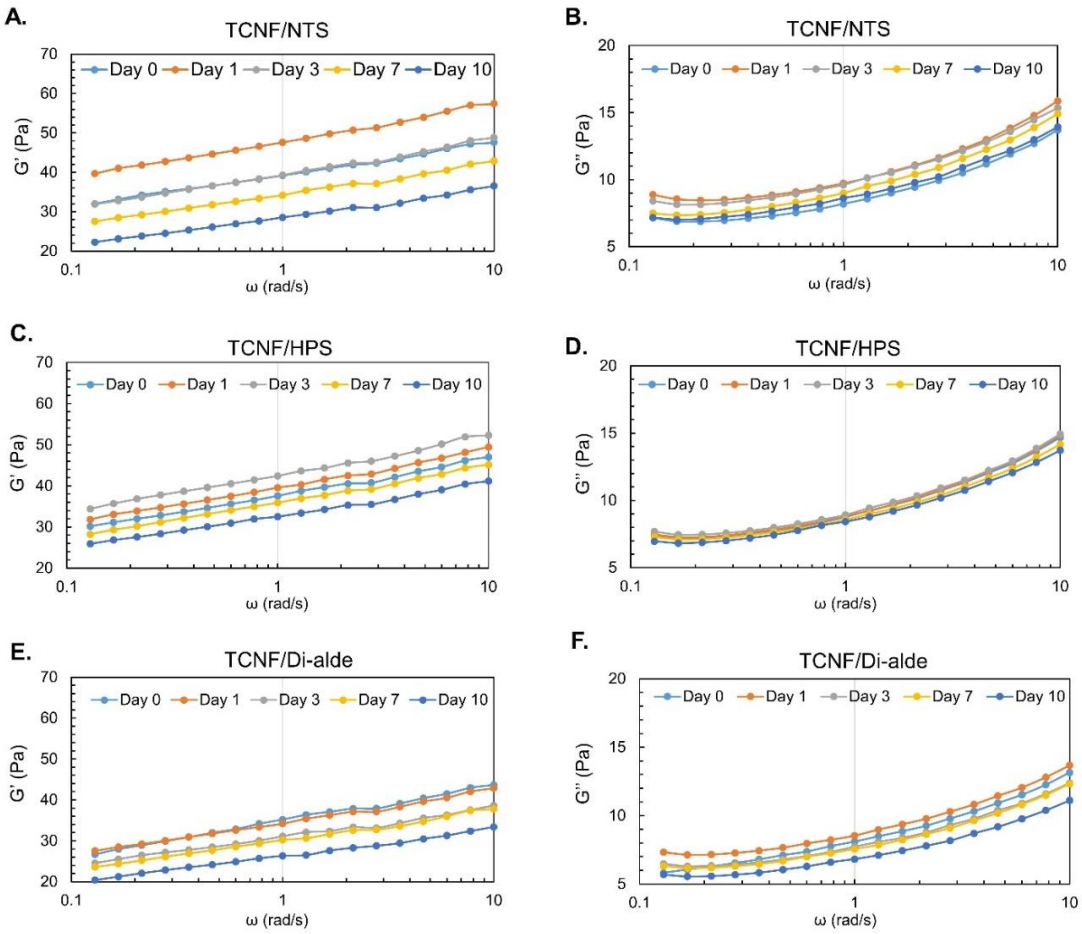

Figure 2-9. Storage moduli (G') and loss moduli (G"), plotted vs. frequency in the 0.1 to 10 rad/s range, for TCNF-modified starch suspensions prepared with different storage-duration starch pastes.

Table 2-3. Storage moduli (G') and loss moduli (G") at the frequency of 1 rad/s, for TCNF-modified starch suspensions prepared with different storage-duration starch pastes.

Starch paste Storage	Storage moduli, G' (Pa)			Loss moduli, G'' (Pa)		
	TCNF/NTS	**TCNF/HPS**	**TCNF/Di-aldS**	**TCNF/NTS**	**TCNF/HPS**	**TCNF/Di-aldS**
Day 0	39.1	37.5	34.1	8.1	8.7	8.1
Day 1	47.5	39.5	35.2	9.7	8.8	8.5
Day 3	39.2	42.4	31.0	9.6	8.9	7.7
Day 7	34.1	35.8	30.2	8.9	8.5	7.5
Day 10	28.5	32.5	26.3	8.6	8.4	6.8

NTS = native tapioca starch, HPS = hydroxypropyl starch, Di-aldS = di-aldehyde starch

The TCNF/NTS suspension exhibited enormous variation of G' with the paste storage duration; however, the TCNF/HPS and TCNF/Di-aldS suspensions exhibited more moderate dependences of G' on the pastes storage time. Reassociated amylose and amylopectin networks in TCNF/NTS suspensions and corresponding hemiacetal crosslinking (after drying) on day 0, on the day with the highest G', and on the day with the lowest G', are shown in **Fig. 2-11**. Surface and cross-section morphology of dried TCNF/NTS film shown in **Fig. 2-10**.

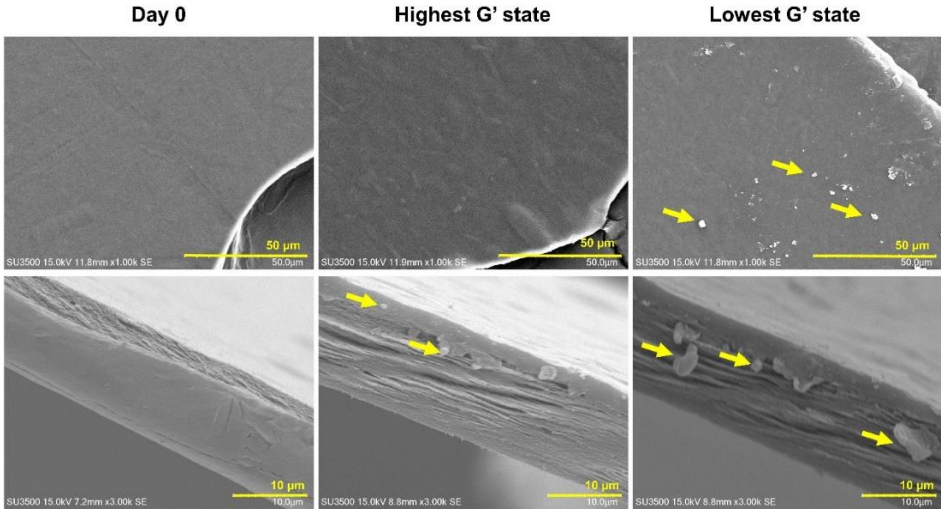

Figure 2-10. Surface and cross-section morphology of dried TCNF/NTS film prepared with suspension at day 0, the day yielding the highest G' and the day yielding the lowest G'. Starch granule on film surface and cross-section indicated by yellow arrow.

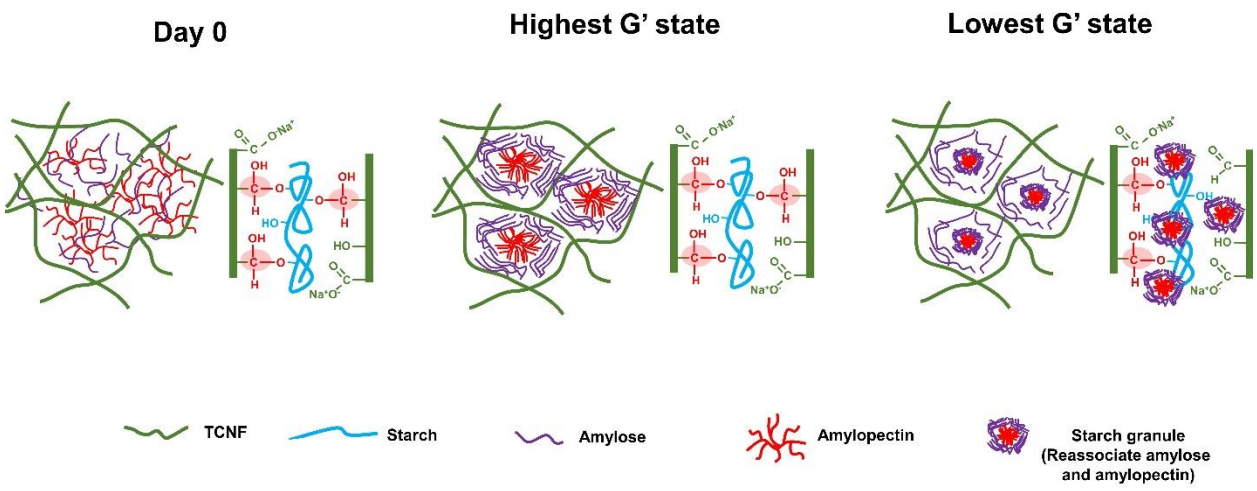

Figure 2-11. Schematic of NTS orientation in TCNF/NTS suspensions on day 0, the day yielding the highest G', and the day yielding the lowest G'. The corresponding hemiacetal crosslinking in dried conditions is shown as well.

On day 0, amylose and amylopectin were randomly arranged in TCNF, and prepared film had smooth surface and cross-section. After a certain storage time, amylose chains started to reassociate and form crystalline arrangements that enhanced the interaction between the starch molecules and TCNF; therefore, TCNF/NTS exhibited the highest G' under these conditions. The hemiacetal crosslinking densities were similar for day 0 and for the day yielding the highest G' state, but owing to higher crystallinity, the film exhibited better mechanical strength and water durability for the highest G' state. Also, dried TCNF/NTS film had smooth surface and small size granule (~ 500 nm – 1 µm) observed in cross-section that contribute to enhance mechanical properties of the film. However, during extended storage, starch granules started to form due to syneresis of the starch paste [30]. The formed granules reduced the interaction between the starch molecules and TCNF, thus reducing G'. In addition, the dried TCNF/NTS film had large size starch granule (~ 5 – 10 µm) on surface and cross-section that diminished mechanical properties of the film. On the other hand, chemical modification of starch slowed the reassociation process, and granule formation took longer than in the native starch. Therefore, TCNF/HPS and TCNF/Di-

aldS exhibited weaker dependence of G' on the paste storage time. Thus, formation of hemiacetal crosslinking and starch paste crystallinity had significant role in enhancing wet strength of TCNF/starch film.

A demonstration of the application of films prepared with the TCNF/HPS suspension (highest G' state) is provided in **Fig. 2-12**. The film thickness was varied by changing the volume of the casting suspension. The TCNF/HPS film possesses adequate mechanical strength (~120 MPa) and optical transparency, which is sufficient for packaging applications. Moreover, it is possible to prepare thick sheets (thickness, ~200 μm). Such thick sheets with self-standing ability can also be used as faceguards; they are promising as substitutes for plastics that are difficult to reuse and must be incinerated from the hygienic point of view.

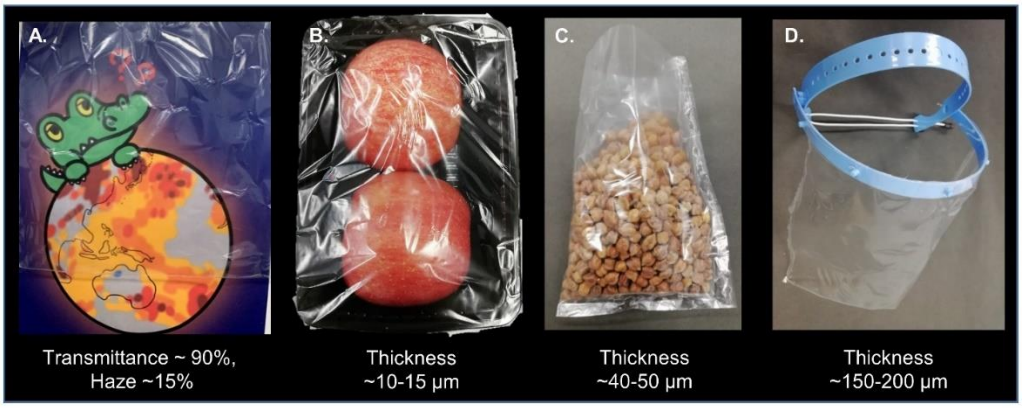

Figure 2-12. (A) TCNF/HPS films exhibit high optical transparency. The film thickness can be optimized according to its use in (B) food packaging covers (~10-15 μm), (C) packaging bags (~40-50 μm), or (D) face shields (~150-200 μm).

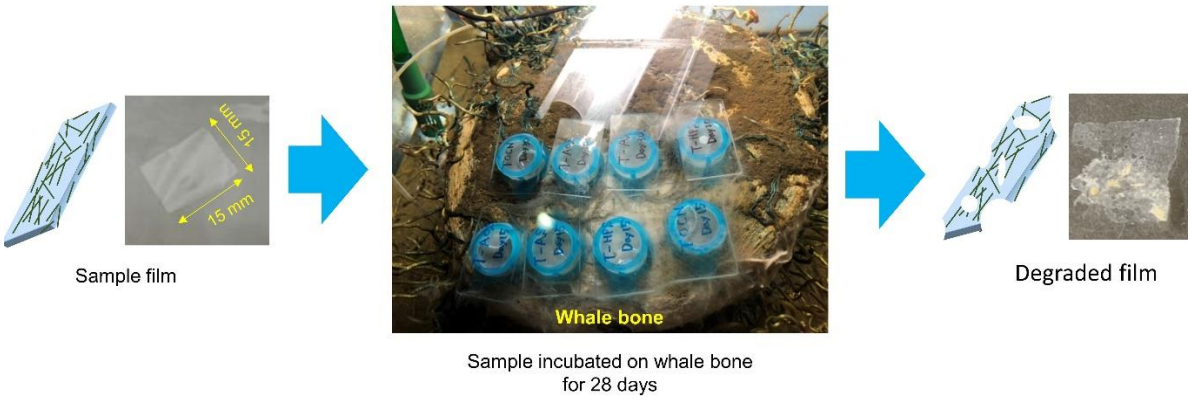

Fig. 2-13. Representation of marine microbial degradation process.

Moreover, TCNF and TCNF/HPS films were kept on a whalebone to confirm the film marine-microbial degradability (**Fig. 2-13**). Surface morphology (after 28 days) is shown in **Fig. 2-14**. TCNF film had less microbial growth and degradability, however, addition of starch (HPS) support microbial growth and enhance degradability. So, TCNF/HPS film had rapid degradation by marine microbes.

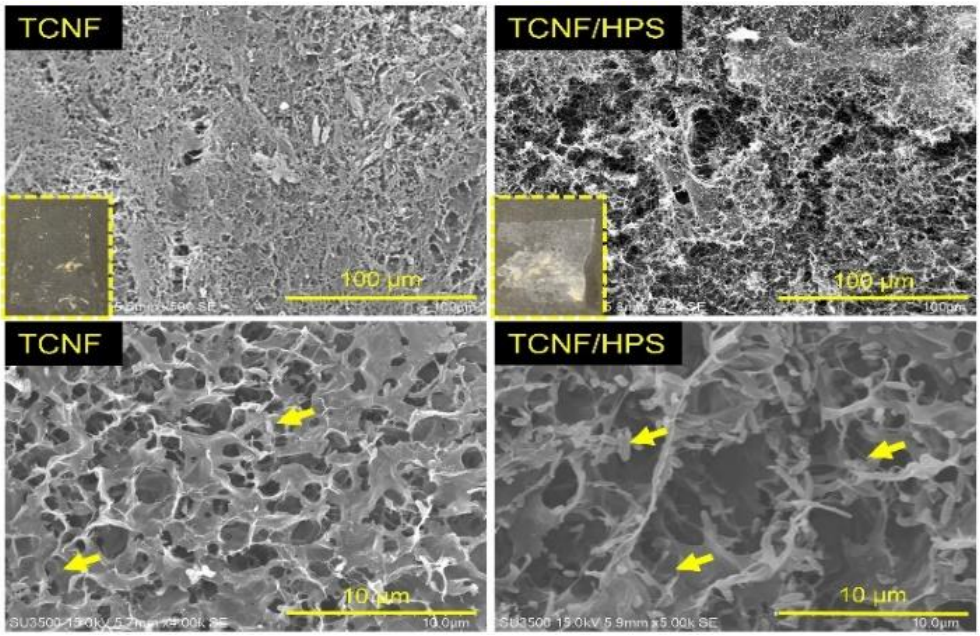

Fig. 2-14. Surface morphology of TCNF and TCNF/HPS films after 28 days kept in marine microbes. Arrows are indicating bacterial growth on the surfaces.

Hence, these results suggest that the optical and mechanical properties and water resistance behavior of TCNF/starch films can be optimized by focusing on starch modification and starch paste crystallinity.

2.4 Conclusions

This study comprehensively analyzed the effect of (NTS, HPS, and Di-aldS) starch paste storage time on the optical, mechanical, and water resistance properties of TCNF/starch films. Short-term storage of starch pastes was found to improve the mechanical and water resistance properties of TCNF/starch films, owing to the synergistic effect of starch paste crystallinity and hemiacetal crosslinking. However, long-term storage of starch pastes promoted the formation of granules that negatively affected the polymer packing and film properties. The TCNF/HPS film prepared using the HPS paste stored for 3 days (~22 $^{\circ}$C, ~25% RH) exhibited adequate strength and durability, making it suitable for packaging applications. Recently, TCNF/HPS composite films have been shown to have good biodegradability in marine environments. Further studies on the marine biodegradability of composite films has conform applicability as marine degradable plastic. We believe that TCNF/HPS films open new vistas for next-generation renewable, water-durable polysaccharide packaging films.

2.5 References

(1) Yaradoddi, J. S.; Hugar, S.; Banapurmath, N. R.; Hunashyal, A. M.; Sulochana, M. B.; Shettar, A. S.; Ganachari, S. V. In *Handbook of Ecomaterials*; Springer International Publishing, **2019**; Vol. 4, pp 2935–2954.

(2) Cornejo-Ramírez, Y. I.; Martínez-Cruz, O.; Del Toro-Sánchez, C. L.; Wong-Corral, F. J.; Borboa-Flores, J.; Cinco-Moroyoqui, F. J. *CyTA - J. Food* **2018**, *16* (1), 1003–1017.

(3) Arayaphan, J.; Boonsuk, P.; Chantarak, S. *Iran. Polym. J. (English Ed.* **2020**, *29* (9), 749–757.

(4) Sun, Q.; Xi, T.; Li, Y.; Xiong, L. *PLoS One* **2014**, *9* (9), e106727.

(5) Vishnuvarthanan, M.; Al Shahidah, M. F.; Gobika, N. R.; Priyadharshini, B.; Rasika, B. *Silicon* **2020**, 1–8.

(6) Han, X.; Chen, S.; Hu, X. *Desalination* **2009**, *240* (1–3), 21–26.

(7) Parra, D. F.; Tadini, C. C.; Ponce, P.; Lugao, A. B. *Carbohydr. Polym.* **2004**, *58* (4), 475–481.

(8) Kulkarni, A. R.; Soppimath, K. S.; Aminabhavi, T. M.; Dave, A. M.; Mehta, M. H. *J. Appl. Polym. Sci.* **1999**, *73* (12), 2437–2446.

(9) Plappert, S. F.; Quraishi, S.; Pircher, N.; Mikkonen, K. S.; Veigel, S.; Klinger, K. M.; Potthast, A.; Rosenau, T.; Liebner, F. W. *Biomacromolecules* **2018**, *19* (7), 2969–2978.

(10) Rhim, J. W.; Gennadios, A.; Weller, C. L.; Carole Cezeirat; Hanna, M. A. *Ind. Crops Prod.* **1998**, *8* (3), 195–203.

(11) Hernández-Muñoz, P.; Villalobos, R.; Chiralt, A. *Food Hydrocoll.* **2004**, *18* (3), 403–411.

(12) Xu, H.; Canisag, H.; Mu, B.; Yang, Y. *ACS Sustain. Chem. Eng.* **2015**, *3* (11), 2631–2639.

(13) Müller, C. M. O.; Laurindo, J. B.; Yamashita, F. *Carbohydr. Polym.* **2009**, *77* (2), 293–299.

(14) Isogai, A.; Saito, T.; Fukuzumi, H. *Nanoscale* **2011**, *3* (1), 71–85.

(15) and, T. S.; Isogai*, A. Wet Strength Improvement of TEMPO-Oxidized Cellulose Sheets Prepared with Cationic Polymers. **2006**.

(16) Isogai, A. *Proc. Jpn. Acad. Ser. B. Phys. Biol. Sci.* **2018**, *94* (4), 161–179.

(17) Soni, R.; Asoh, T. A.; Uyama, H. *Carbohydr. Polym.* **2020**, *238*, 116203.

(18) Guo, L.; Du, X. *Starch - Stärke* **2014**, *66* (9–10), 887–894.

(19) Putaux, J. L.; Buléon, A.; Chanzy, H. *Macromolecules* **2000**, *33* (17), 6416–6422.

(20) Wang, S.; Li, C.; Copeland, L.; Niu, Q.; Wang, S. *Compr. Rev. Food Sci. Food Saf.* **2015**, *14* (5), 568–585.

(21) Alcázar-Alay, S. C.; Meireles, M. A. A. *Food Sci. Technol.* **2015**, *35* (2), 215–236.

(22) Oh, S. M.; Kim, H. yun; Bae, J. E.; Ye, S. J.; Kim, B. Y.; Choi, H. D.; Choi, H. W.; Baik, M. Y. *Food Sci. Biotechnol.* **2019**, *28* (6), 1723–1731.

(23) Santana, J. S.; de Carvalho Costa, É. K.; Rodrigues, P. R.; Correia, P. R. C.; Cruz, R. S.; Druzian, J. I. *J. Appl. Polym. Sci.* **2019**, *136* (4), 47001.

(24) Ishiguro, K.; Noda, T.; Kitahara, K.; Yamakawa, O. *Starch - Stärke* **2000**, *52* (1), 13–17.

(25) Haq, F.; Yu, H.; Wang, L.; Teng, L.; Haroon, M.; Khan, R. U.; Mehmood, S.; Bilal-Ul-Amin; Ullah, R. S.; Khan, A.; Nazir, A. *Carbohydrate Research*. Elsevier Ltd April 1, 2019, pp 12–35.

(26) Shi, Y. C.; Seib, P. A. *Carbohydr. Res.* **1992**, *227* (C), 131–145.

(27) Maloney, T. C. *Holzforschung* **2015**, *69* (2), 207–213.

(28) Fonseca, L. M.; Gonçalves, J. R.; El Halal, S. L. M.; Pinto, V. Z.; Dias, A. R. G.; Jacques, A. C.; Zavareze, E. da R. *LWT - Food Sci. Technol.* **2015**, *60* (2), 714–720.

(29) Kitamura, S.; Yoneda, S.; Kuge, T. *Carbohydr. Polym.* **1984**, *4* (2), 127–136.

(30) Yousif, E. I.; Gadallah, M. G. E.; Sorour, A. M. *Ann. Agric. Sci.* **2012**, *57* (1), 19–27.

Chapter 3

A facile way to prepare fresh water durable and marine degradable cellulose nanofiber reinforced starch film

3.1 Introduction

Cellulose and starch are hydrolysis via the enzymatic route is accomplished synergistically by actions of a group of enzymes known as cellulases and amylase[1,2]. Marine microbes are potential source of such enzymes, therefore, packaging bags prepared by biomass (cellulose and starch) are better substitute for marine degradable single-use plastic[3,4]. However, poor freshwater durability of cellulose and starch based films restrict their applications.

Many chemically modified cellulose as cellulose acetate, cellulose octanoate, cellulose palmitate, and methylcellulose have been prepared to improve cellulose film's water durability[5,6]. Such hydrophobic modification was found to enhance water durability; however, enzymatic degradation was drastically reduced. Almost zero hydrolysis rate for cellulose acetate, cellulose octanoate, cellulose palmitate by enzymatic degradation has been reported in the earlier study[7,8]. Many polymers such as poly(acrylamide) (PAM), poly(vinylamine) (PVA), and poly(ethyleneimine) (PEI) have been introduced to cellulose to improve its wet tensile strength[9–11]. However, these synthetic polymers are non-degradable and hazardous to the environment. On the other hand, starch is biocompatible, biodegradable, renewable, and is an abundant polysaccharide. Blending of starch with serval polymers as PVA, PLA, PHB, PCL etc. enhanced

mechanical properties and degradability in marine environment[12–14]. However, fresh water durability reduced owing to hydrophilicity of starch.

Aldehydes might be the most frequently used chemicals for starch crosslinking due to their high reaction efficiency to form hemiacetal/acetal crosslinking[15]. Aldehyde moieties introduced to polysaccharides to prepare environmental friendly cross linkers. Starch film cross-linked by di-aldehyde sucrose had water stability compare to non-cross-linked neat starch film. PVA/di-aldehyde starch composite film had higher freshwater durability owing to hemiacetal crosslinking[16–18]. Blending of starch with TEMPO-oxidized cellulose nanofiber (TCNF) enhanced water durability and strength owing to provide flexible hemiacetal binding between TCNFs[19,20]. Therefore, hemiacetal crosslinking had a crucial role to enhance fresh water durability of starch base composite films. However, cellulose/starch composite film's freshwater durability and strength are still needed to improve for packaging application.

In chapter 3, sodium periodate oxidation was performed to cellulose nanofiber (Selectively convert the two secondary hydroxyl groups in the C2 and C3 position of the anhydroglucose units into aldehyde moieties)[21]. The oxidation time was optimized to prepare film with adequate mechanical strength. Further, we demonstrated that the addition of starch in oxidized cellulose nanofiber enhances the water durability and strength due to hemiacetal crosslinking. Moreover, a degradation test was performed in marine mud and marine microbes to confirm the film's marine degradability. Thus, the development of polysaccharides-based freshwater durable and the marine-degradable film will potentially substitute for next-generation packaging material to reduce global environmental effects.

3.2 **Experimental section**

Materials

Commercially available cellulose powder was supplied by Nacalai Tesque, Japan. Sodium periodate and ethylene glycol were purchased from Fujifilm Wako, Japan. Phosphate buffer saline (pH 6) was provided by Nacalai Tesque, Japan. Sodium azide was purchased from Sigma Aldrich, Japan. Cellulase enzyme (*Aspergillus niger)* was supplied by TCI, Japan. All reagents were laboratory grades. Three types of modified tapioca starch powder, hydroxypropyl starch (HPS, DS: 0.05) and di-aldehyde starch (Di-aldS, Molar substitute 5.4 (A) and 15.2 (B)) was supplied by Nihon Shokuhin Kako Co. Ltd., Japan and used as received. Milli-Q water was used throughout the experiment.

Preparation of MCNF suspension

We prepared a dispersion of cellulose powder (~1% w/v) in water. The dispersion was processed by wet pulverization process, subject to mechanically disintegrate cellulose into cellulose nanofiber. In the disintegration process, the dispersion was pressurized at approximately 245 MPa and ejected into the device chamber through a 100 μm aperture nozzle, then pulverized with a ceramic ball using a Star Burst Mini wet pulverizing and dispersing device (Sugino Machine Co., Ltd., Japan) equipped with a ceramic ball collision chamber[22]. The disintegration process repeated around ~ 25 times to get fibrillated and homogeneous suspension of cellulose nanofiber. The prepared suspension was named mechanically fibrillated cellulose nanofiber (MCNF) in the experiment. The concentration of MCNF suspension was calculated by weight measurement before and after lyophilization.

Preparation of starch paste

Hydroxypropyl starch (HPS) powder (5.0 g) was added to 100 mL of Mili-Q water. The dispersion was mixed using magnetic stirring at 90 °C for 1 h to obtain a homogeneous starch paste. The prepared paste was stored at room temperature for further experiments.

Preparation of OMCNF and OMCNF/HPS suspension

In a close container, 20 g MCNF suspension (~ 1%, w/v) dispersed in water (20 ml). 0.4 g (2-time weight of MCNF) of sodium periodate added in the homogeneous dispersion and mixed by magnetic stirrer for 1 h at room temperature (~28 °C). After 1 h, the remaining periodate was decomposed by adding excess ethylene glycol[23]. Further, the dispersion was thoroughly washed with water (at least 5 times wash). The final concentration of OMCNF was measured by the freeze-drying process. Aldehyde moieties concentration measured by DNPH test. Prepared OMCNF suspension (~0.8%, W/V) and HPS paste (5%, W/V) were blended together in different HPS concentrations and stirred until a homogeneous dispersion was obtained, and named OMCNF/HPS suspension.

Preparation of films

Prepared MCNF, OMCNF, and OMCNF/HPS suspension (~1%, W/V) were cast in a Teflon PFA Petri dish and kept in an oven at 45 °C for 6 h. Dried films were cut into specimens for further experiments.

Aldehyde concentration measurement

Aldehyde group concentration in OMCNF suspension was measured by the UV-spectrophotometric method using 2,4-dinitrophenylhydrazine (DNPH). 5 mg of DNPH was dissolved in 0.2 mL of concentrated sulphuric acid and stirred to obtain a homogeneous solution.

2 mL of ethanol was added under continuous stirring at room temperature. The mixture was allowed to react for 10 min to achieve homogenization. The final volume was made up to 20 mL by adding water. Prepared DNPH solution was diluted by water into four different concentrations, and absorbance at 360 nm was measured for each concentration using a spectrophotometer. A calibration curve for DNPH was plotted to formulate a standard equation for aldehyde concentration measurement.

500 µL of OMCNF was added to 5 ml of the prepared DNPH solution, and the mixture was allowed to react for 5 h at room temperature. Unreacted DNPH was collected by centrifugation, and absorbance was measured at 360 nm using the spectrophotometer. The amount of aldehyde moieties was calculated as:

$$\text{Aldehyde concentration (µmol/g)} = \frac{\text{Reacted DNPH concentration (µmol)}}{\text{Amount of celluose in OMCNF (g)}}$$

Enzymatic degradation test

Fast biodegradation of the films was measured in laboratory conditions by enzymatic hydrolysis. Commercially available cellulase enzyme (activity 6000 unit/g) dissolved in phosphate buffer saline (0.1 mol/l, pH 6). Sodium azide (0.1 g) is used as an anti-bacterial agent. The films were cut into small pieces (10 mm × 10 mm) and placed in a six-well plate. The needed enzyme mixture was added based on the dry weight of the films according to the equation[7]

$$\text{Volume of enzyme mixture} = \frac{50\left(\frac{FPU}{g}\right) \times dry\ weight\ of\ film\ (g)}{Activity\ of\ prepared\ enzyme\ mixture\ \left(\frac{FPU}{ml}\right)}$$

Five days incubation was started with the addition of the enzyme mixture at 37 °C. Three replicates of each sample were measured. As a reference, films were kept in PBS solution without enzyme. After the hydrolysis, the remaining film samples were gently taken out with the help of tweezers, washed with ethanol, and followed by the drying process. Percentage weight loss was calculated as

$$\text{Percentage weight loss (\%)} = \frac{W_{BD} - W_{AD}}{W_{BD}} * 100$$

Where, W_{BD} and W_{AD} are weights of the dried films before degradation and after degradation, respectively.

Marine microbial degradation test performed same as explain in **chapter 2**.

Characterization

Lyophilized MCNF and OMCNF suspensions were analyzed by Fourier transform infrared spectra (Thermo scientific, Nicolet iS5) to confirm the oxidation and date analyzed by OMNIC software. The mechanical properties of the films were evaluated by a tensile test. Five specimens (20 mm × 5 mm) were cut from each film. A micrometer was used to measure their thickness before the test. Measurements were taken at four different positions for each specimen, and the average value was used for the calculation. Tensile test was performed using a universal testing machine (EZ graph, Shimadzu Corporation, Japan) with a 100 N load cell and a 1 mm/min strain rate. Water uptake ratio (WUR) test was performed in freshwater. Dried film specimens (2 cm × 2 cm) were immersed in water. After a fixed time, swollen samples were gently taken out using tweezers, and excess water was removed with tissue paper before samples were weighed. WUR was calculated as follows:

$$\text{WUR (\%)} = \frac{W_{ss} - W_{ds}}{W_{ds}} * 100$$

where W_{ds} and W_{ss} are weights of the dried and swollen samples, respectively.

The tensile test of swollen membranes was performed using a universal testing machine with a 10 N load cell and 1 mm/min strain rate. Three samples were taken from each group for measurement, and the average value of the calculation is reported. Surface morphology of the marine degraded samples was observed by SEM (Hitachi SU3500, Japan) at an accelerating voltage of 15 kV and a working distance of 10 mm. Before the SEM examination, the surface was sputter-coated with platinum-palladium (5 nm thickness) using a vacuum sputtering instrument (Magnetron sputter MSP-1S, Japan).

3.3 Result and discussion:

Optimization of water durability

To fabricate high water durable film, Cellulose nanofiber suspension was prepared by wet pulverization process (245 MPa, 25 Passes) and named mechanically fibrillated cellulose nanofiber (MCNF). Further, MCNF was followed by sodium periodate oxidation ($NaIO_4$) to prepare oxidized cellulose nanofiber (OMCNF) suspension. The prepared suspensions were converted into films by solvent casting method, as shown in **Fig. 3-1**.

Oxidation was optimized to get adequate mechanical strength of dried OMCNF film. Oxidation of MCNF suspension performed for 15 min, 1 h, and 4 h (at constant temperature 28 °C and oxidant concentration) and named as Run 1, Run 2 and Run 3, respectively. During oxidation, aldehyde moieties are introduced to the surface of cellulose nanofiber that forms di-aldehyde cellulose. FTIR spectra of MCNF and OMCNF (different times oxidized) are shown in **Fig. 3-2A**. MCNF had O-

H stretching (adsorbed water signal) peak at 1641 cm^{-1}. After oxidation, a weak carbonyl (C=O) stretching vibration peak was observed at 1732 cm^{-1} and O-H stretching peak shifted to 1635 cm^{-1}. With higher oxidation time, the O-H stretching peak intensity (1635 cm^{-1}) was reduced, and the carbonyl stretching peak intensity increased. That confirms the convergence of hydroxyl moieties (at C2 and C3) to aldehyde moieties.

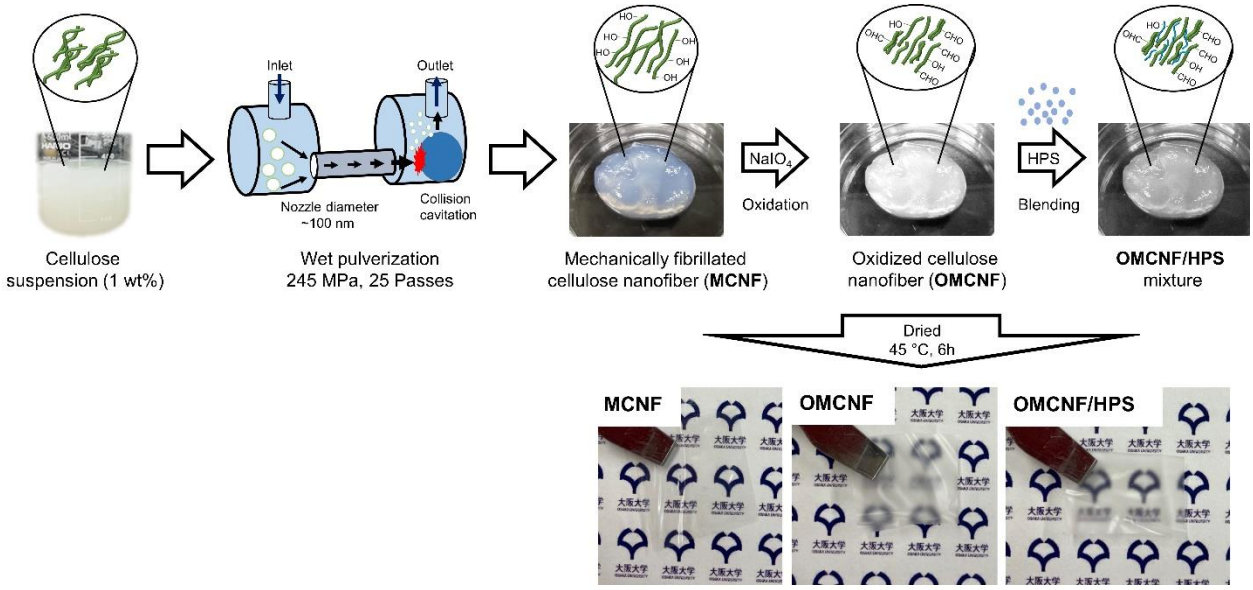

Figure 3-3. Illustrative representation of MCNF, OMCNF and OMCNF/HPS films preparation process.

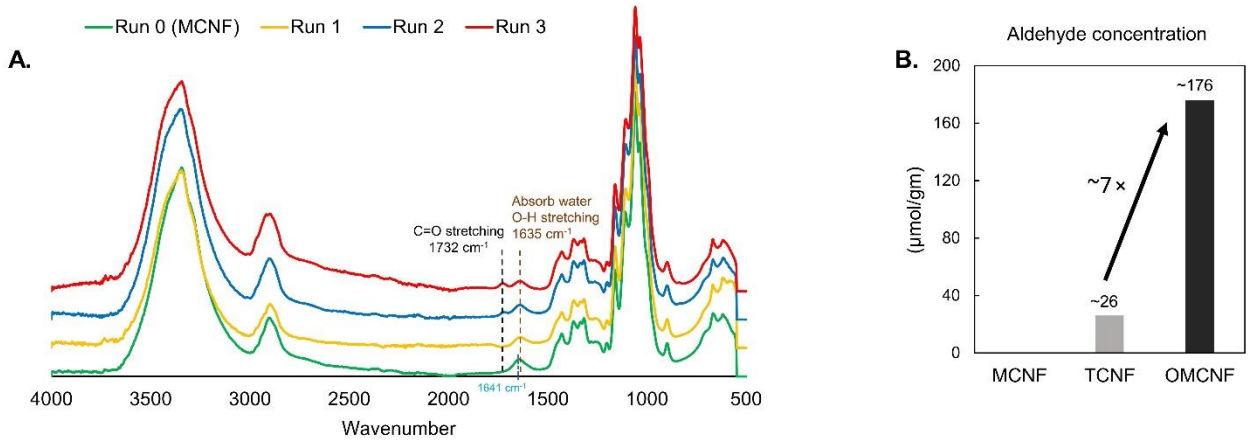

Figure 3-2. (A) FTIR spectra of different time oxidized OMCNF and (B) comparative analysis of aldehyde moieties on MCNF, TCNF and 1 h oxidized OMCNF.

Aldehyde concentration was calculated as 39, 176 and 887 µmol/g for Run 1, 2, and 3, respectively. The prepared self-standing OMCNF films were shown in **Fig. 3-3A**, and MCNF film (named as Run 0) used as control. *UV-vis spectra* of self-standing MCNF and OMCNF films are shown in **Fig. 3-3C,** and the transmittance at 650 nm was used as the relative value for comparison, and data are summarized in **Table 1**. Transmittance of MCNF film was 68% that was drastically reduced to 43%, 26%, and 14% with higher oxidation time. Tensile strength and strain energy density of dried OMCNF films are shown in **Fig. 3-3D, E** and summarized in **Table 1**. MCNF film had a tensile strength of 175 MPa and a strain energy density of 1.99 MJ/m^3. However, OMCNF films exhibited a tensile strength of 117, 99, and 65 MPa, and strain energy density of 1.09, 0.84 0.49 MJ/m^3, for Run 1, Run 2 and Run 3, respectively. Thus, optical transparency, tensile strength, and strain energy density of dried OMCNF films rapidly reduced with higher oxidation.

Morphology of surface and cross-section were showed in **Fig. 3-3B**. MCNF film had a smooth surface and cross-section, indicating good packaging of fibers. However, the OMCNF films surface and cross-section become rough owing to agglomerate fibers, and roughness was increasing with higher oxidation. Then, non-uniform agglomerate fibers disturbed packaging and reduced the optical transparency. Moreover, during oxidation, cellulose nanofiber gets depolymerized, fibers crystallinity diminished, and crystallinity reduction is continued with the oxidation. Therefore, Strain energy density of the films was rapidly reduced. With Run 1, the prepared OMCNF film had a smooth surface with adequate mechanical strength. Furthermore, aldehyde moieties concentration was found to be ~176 µmol/g that was almost ~7 times higher than aldehyde concentration of TEMPO-oxidized cellulose nanofiber (~26 µmol/g) as shown in **Fig. 3-2B**. Therefore, OMCNF film prepared with 1 h oxidation was quite suitable for further experiment.

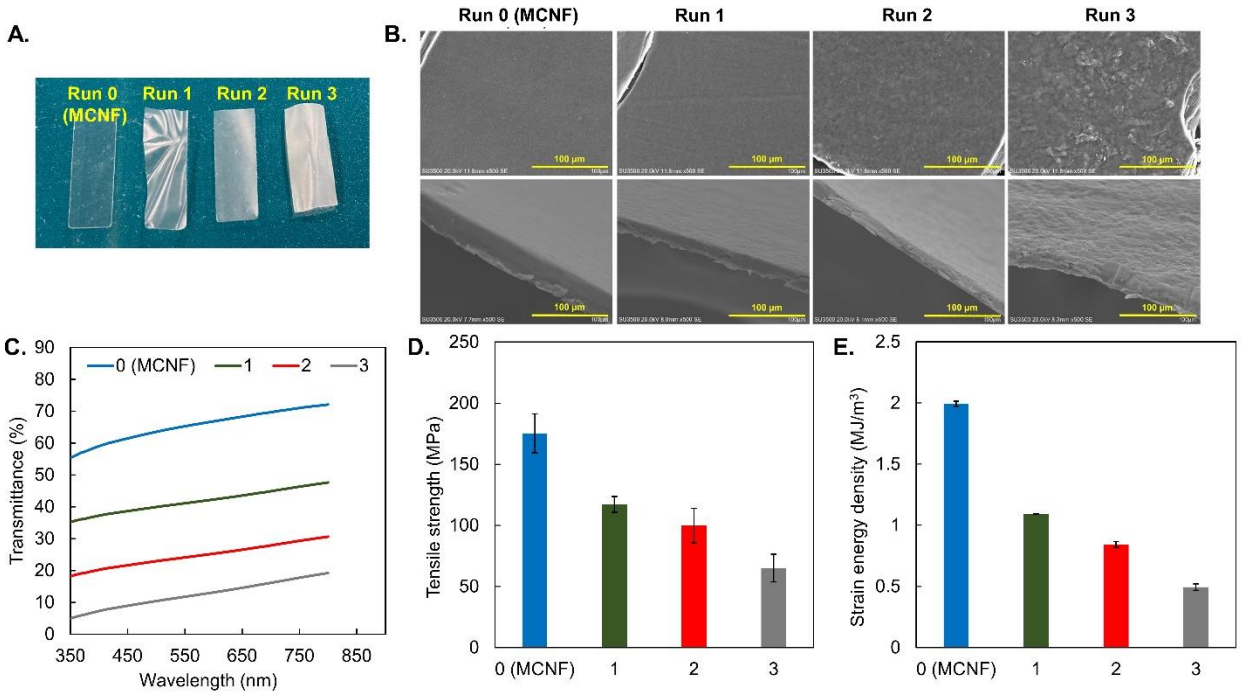

Figure 3-3. Characterization of different time oxidized cellulose nanofiber (OMCNF) films as (A) self-standing films (B) surface and cross-section morphology (C) UV-spectra in visible wavelength region (D) tensile strength and (E) strain energy density.

Table 1. Dried film optical transparency and mechanical properties of different time oxidized cellulose nanofiber films.

Run groups	Oxidation* time	Aldehyde (µmol/g)	Optical transparency (%) (at 650 nm)	Tensile modulus (GPa)	Tensile strength (MPa)	Strain (%)	Strain energy density (MJ/m^3)
0 (MCNF)	-	0	68	8.24±1.71	175±15	2.27±0.26	1.99±0.020
1	15 min	39	43	7.87±0.75	117±6	1.86±0.12	1.09±0.039
2	1 h	176	26	6.87±1.33	99±14	1.68±0.32	0.84±0.022
3	4 h	887	14	5.79±1.27	65±11	1.52±0.43	0.49±0.026

* Temperature (28 °C) and oxidant concentration was constant during reaction.

To analyze wet durability, prepared MCNF and OMCNF films kept in water. The water uptake profile for the films is shown in **Fig. 3-4A**. MCNF and OMCNF films exhibited ~ 207% and ~53% water update ratio (WUR), respectively. Rapid reduction observed in WUR of OMCNF film. OMCNF was blended with HPS to further improve water durability. The WUR of OMCNF/HPS films prepared with different concentrations of HPS (with respect to OMCNF) is shown in **Fig. 3-4B**. OMCNF/HPS film prepared with ~64% HPS concentration exhibited ~122% WUR. With reducing the HPS concentration to ~32% and ~16%, the WUR decreased to ~83% and ~65%, respectively. OMCNF/HPS film prepared with ~8% HPS concentration showed a minimum WUR of ~30%, significantly lower than OMCNF film.

Water uptake profile and wet tensile strength of MCNF, OMCNF, and OMCNF/HPS films measured after 2 h immersion in water, are shown in **Fig. 3-5** and data summarized in **Table 3-2**. MCNF film had a tensile strength of 1.62 MPa with 27.8 kJ/m^3 strain energy density. Wet tensile strength increased to 20.4 and 35.8 MPa, and strain energy density was enhanced to 373.9 and 646.1 kJ/m^3 for OMCNF and OMCNF/HPS films, respectively.

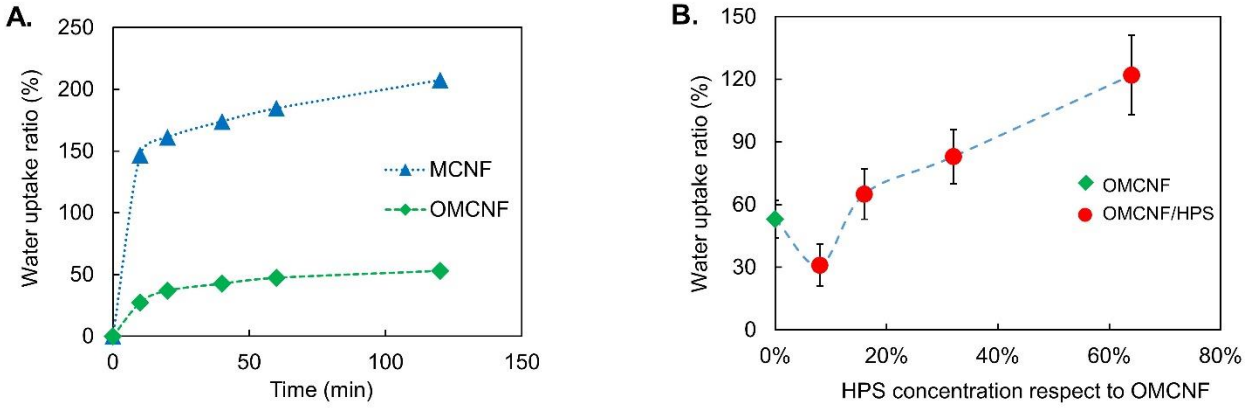

Figure 3-4. (A) Water uptake profile of MCNF and OMCNF films and (B) water uptake ratio of OMCNF and OMCNF/HPS films (Prepared with different HPS concentration) after 2 h immersion in fresh water.

Aldehyde moieties on OMCNF form inter and intra molecular hemiacetal bond during the drying process of film preparation. This hemiacetal crosslinking improved the water durability of OMCNF film (**Fig. 3-5C**); therefore, OMCNF film showed a reduced water uptake ratio of ~53% and higher wet tensile strength of 20.4 MPa. The addition of HPS works as a flexible binder between OMCF and HPS. Also, the higher reactivity of hydroxypropyl moieties enhanced hemiacetal crosslinking density. Therefore, OMCNF/HPS film had a minimum WUR of ~31% and the highest wet strength and strain energy density. Wet strength demonstration of OMCNF/HPS film shown in **Fig. 3-5D**. Moreover, HPS granule observed in cross-section (**Fig. 3-6**) that enhanced inter and intra fiber interaction, reduced mobility and increased rigidity. So, dried OMCNF/HPS film had higher tensile strength (~117 MPa) than OMCNF film (**Fig. 3-6**). However, access HPS concentration increased WUR owing to the hydrophilicity of starch.

To confirm the effect of hemiacetal crosslinking, Di-aldehyde starch (different D.S.) blended with MNCF to prepare MCNF/Di-aldS films. Wet films stress-strain curves and corresponding strain energy density are shown in **Fig. 3-7**. Wet film mechanical properties (stress and strain) elevated, and strain energy density enhanced to 0.98, 30, and 68 kJ/m^3 for MCNF, MCNF/Di-aldS_A, and MCNF/Di-aldS_B, respectively.

Table 3-2. Dried and wet film mechanical properties of MCNF, OMCNF and OMCNF/HPS films.

Type of film	Dried film mechanical properties		Wet film mechanical properties		
	Tensile modulus (GPa)	Tensile strength (MPa)	Tensile modulus (MPa)	Tensile strength (MPa)	Strain energy density (kJ/m^3)
MCNF	8.24±1.71	175±15	56±9	1.62±0.8	27.8±11.4
OMCNF	6.87±1.33	99±14	786±139	20.4±5.7	373.9±83.4
OMCNF/HPS	7.87±0.75	117±13	1479±498	35.8±5.2	646.1±136.2

Water durability increases with the di-aldehyde substitute in starch, confirming the hemiacetal crosslinking role to elevate the film's wet strength. However, the reactivity of hydroxypropyl is higher to form crosslinking, and high mobility and flexibility of starch (compare to cellulose) elevated crosslinking density. So, OMCNF/HPS film had a significantly high wet strain energy density (646 kJ/m^3) than MCNF/Di-aldS film (68 kJ/m^3). In addition, loosely bonding starch in MNCF/Di-aldS film was found to show adhesive behavior (application demonstration of adhesive behavior shown in **Fig. 3-8,** indicating lesser reactivity of hydroxyl moieties (MCNF) to interact with di-aldehyde starch.

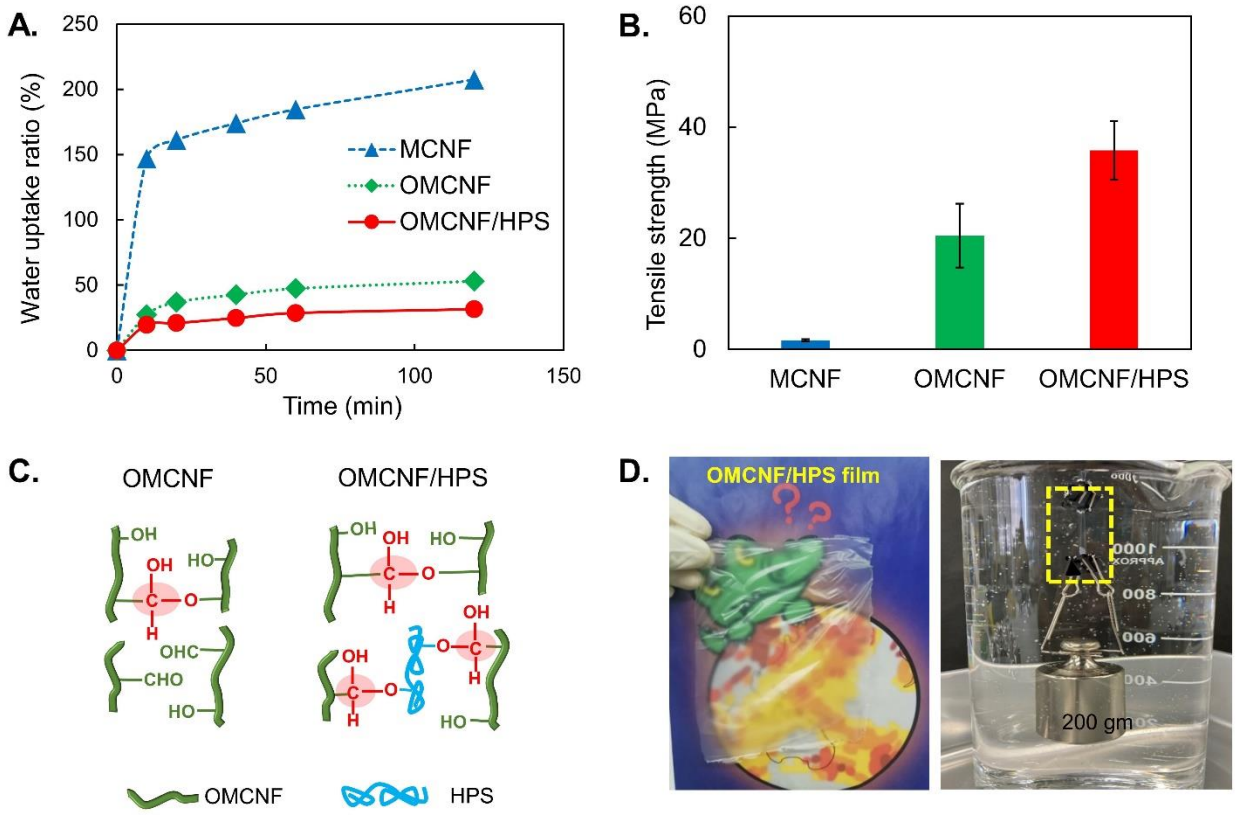

Figure 3-5. (A) Water uptake profile of MNCF, OMCNF and OMCNF/HPS films and (B) Wet tensile strength of these films after 2 h immersion in water. (C) Possible formation of hemiacetal crosslinking that elevated the wet strength of the films. (D) Demonstration of large size self-standing OMCNF/HPS film and wet strength of the film. OMCNF/HPS film used for wet strength demonstration highlighted by Yellow Square.

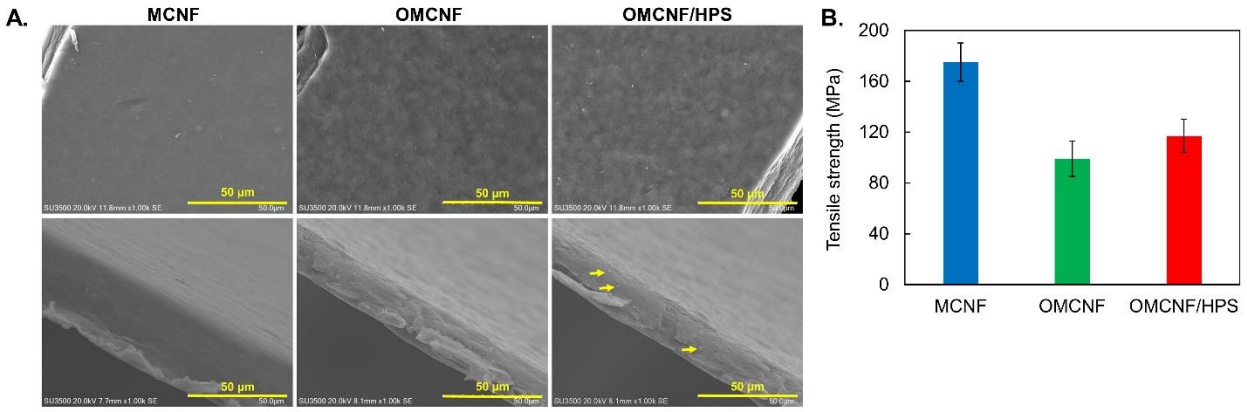

Figure 3-6. (A) Dried film surface/cross-section morphology and (B) tensile strength of MCNF, OMCNF and OMCNF/HPS.

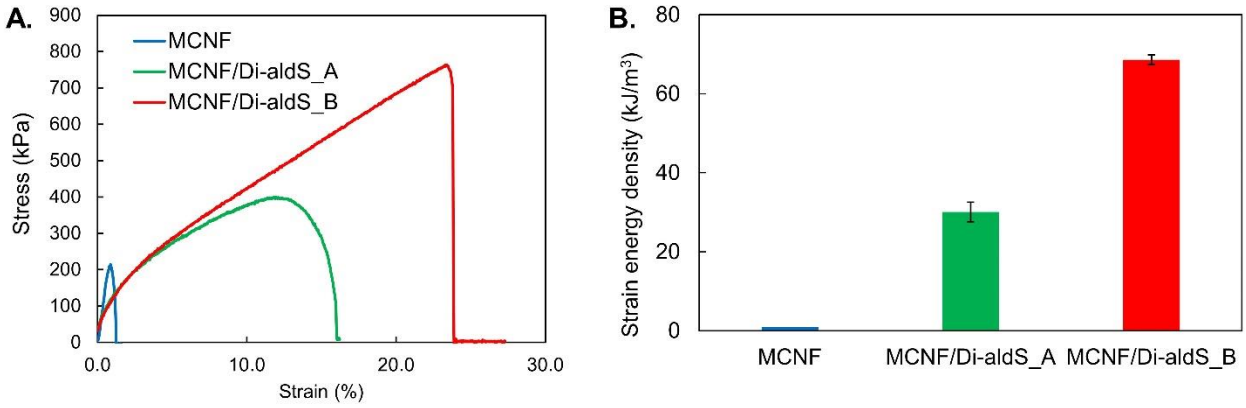

Figure 3-7. Wet films (A) stress-strain curves and corresponding (B) strain energy densities of MCNF and MCNF/Di-aldS films (prepared with different D.S. of di-aldehyde moieties in starch).

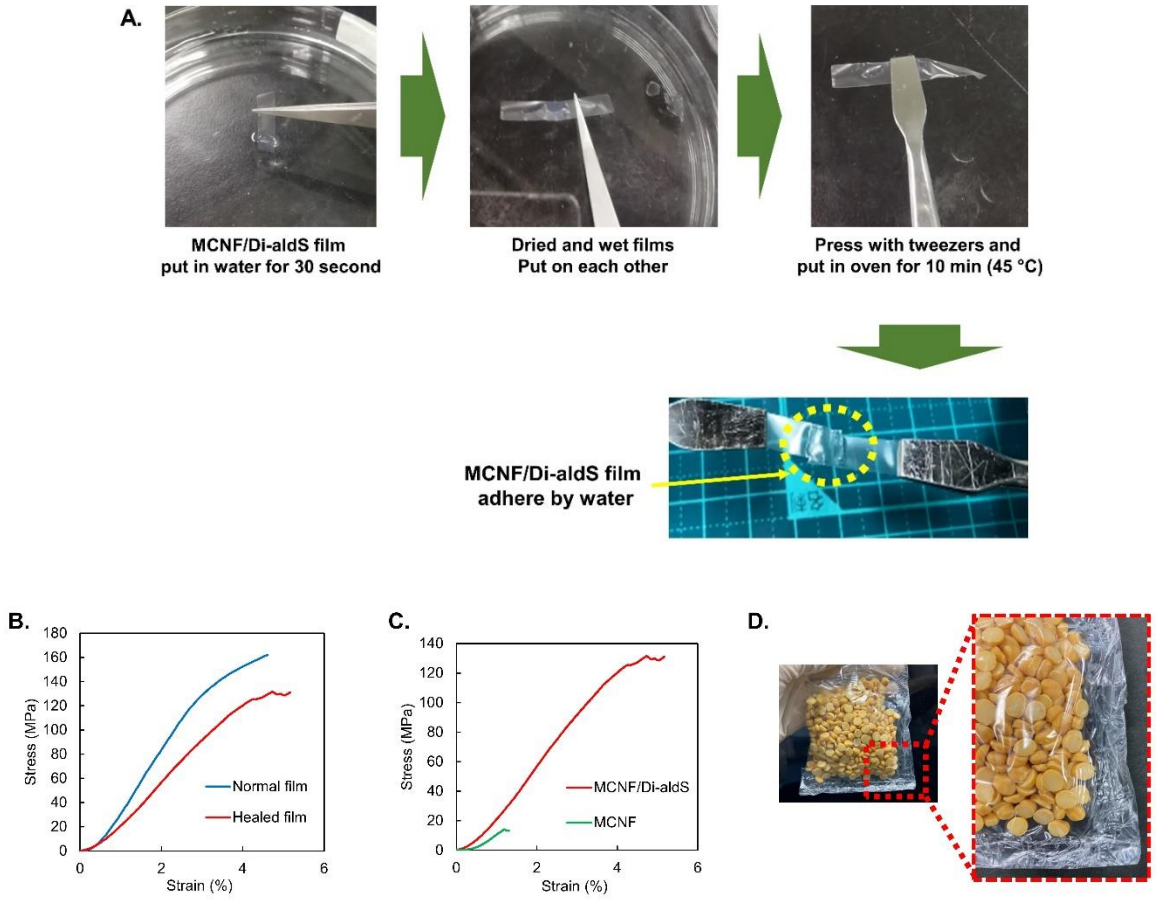

Figure 3-8. (A) Representation of water healing behavior of MCNF/Di-aldS film. (B) Stress-strain curve of MCNF/Di-aldS, normal film and healed film and (C) role of Di-aldS in recovery of healed film mechanical properties. (D) Application demonstration of MNCF/Di-aldS film healing behavior in packaging.

These results suggest hemiacetal crosslinking has a crucial role in the water durability of OMCNF and OMCNF/HPS films. Also, the addition of starch enhanced hemiacetal crosslinking density and elevated wet strength of the films. Aldehyde moieties on CNF and hydroxypropyl moieties on starch are a good combination for high wet strength films, instead of vice-versa.

Degradability of the films

MCNF, OMCNF, and OMCNF/HPS films degradation test were performed in the artificial marine environment. Sample preparation for marine microbial degradation had explained above, and illustrative representation is shown in **chapter 2** (**Fig. 2-13**).

MCNF, OMCNF, and OMCNF/HPS films were kept on a whalebone to confirm the film marine-microbial degradation. Surface morphology (after 28 days) is shown in **Fig. 3-9**. MCNF film shown rapid marine microbial degradation; however, OMCNF film had less bacterial growth and slow degradation. OMCNF/HPS had shown high bacterial growth with moderate degradation that was higher compare to OMCNF film. These results suggest that non-chemically modify cellulose had rapid degradation by marine microbes. Also, the addition of starch supports microbial growth on the film surface that helps to enhance degradation.

Effect of chemical modification on enzymatic degradation analyzed by keeping the film in cellulase enzyme at laboratory conditions. Percentage weight loss of MCNF, OMCNF, and OMCNF/HPS films after 5 days immersion in cellulase enzyme are shown in **Fig. 3-10**. MCNF film had shown ~90% weight loss; however, OMCNF and OMCNF/HPS film had shown almost similar weight loss of ~75%. Thus, oxidized cellulose films had slow degradation due to chemical modification. Slow hydrolysis rate for oxidized cellulose by enzymatic hydrolysis has also been reported in an earlier study[24,25]. Also, The portion for glucose released was reduced with longer oxidation time; therefore, 1 h oxidation was quite suitable for adequate degradability.

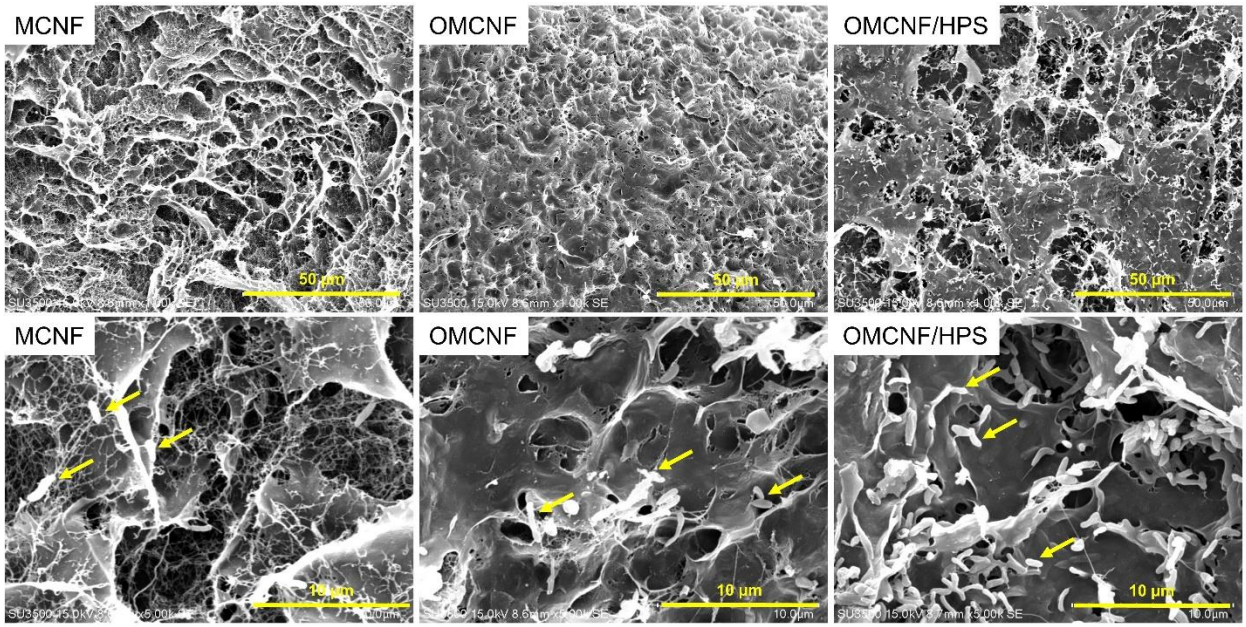

Figure 3-9. Surface morphology of MCNF, OMCNF and OMCNF/HPS films after 28 days kept in marine microbes. Arrows are indicating bacterial growth on the surface.

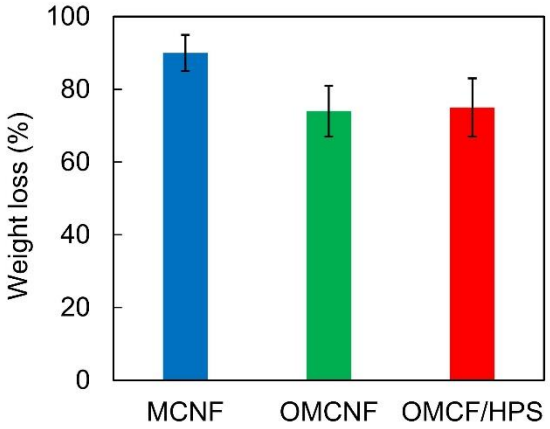

Figure 3-10. Weight loss (%) of MCNF, OMCNF and OMCNF/HPS films after 5 days immersion in cellulase enzyme at 37 °C.

Therefore, OMCNF/HPS film prepared with 1 h oxidized cellulose nanofiber had high fresh water durability with adequate marine microbial degradability. These results suggest that the water

durability and marine degradability of OMCNF/HPS films can be optimized by optimize the cellulose oxidation time and starch concentration.

3.4 Conclusion

This study comprehensively studied the freshwater durability and marine degradability of sodium periodate oxidized cellulose nanofiber (OMCNF) film. The film prepared with 176 μmol/g aldehyde concentration (1 h oxidation) had adequate dried and wet film mechanical properties. Further, the film water durability could be enhanced by the addition of starch (hydroxypropyl starch, HPS). The formation of hemiacetal crosslinking between oxidized cellulose nanofiber and starch elevated water durability of OMCNF/HPS film. Aldehyde moieties on CNF and hydroxypropyl moieties on starch are good combination for high wet strength films, instead of vice-versa. Moreover, starch addition enhanced microbial growth that increased OMCNF/HPS film's degradability in marine conditions. We believe that the OMCNF/HPS film opens the research for the next generation freshwater durable, marine-degradable, renewable, and high-performance - green packaging film.

3.5 References

(1) Kumar, D.; Murthy, G. S. *Biotechnol. Biofuels* **2013**, *6* (1), 63.

(2) M. Itävaara, M. Siika-aho, L. Viikari. *Journal Of Environmetal Polymer Degradation*; **1999**; Vol. 7. pp 67-73.

(3) Trivedi, N.; Reddy, C. R. K.; Lali, A. In *Advances in Food and Nutrition Research*; Academic Press Inc., 2016; Vol. 79, pp 27–41.

(4) Song, J. H.; Murphy, R. J.; Narayan, R.; Davies, G. B. H. *Philos. Trans. R. Soc. B Biol. Sci.* **2009**, *364* (1526), 2127–2139.

(5) Havimo, M.; Jalomäki, J.; Granström, M.; Rissanen, A.; Iivanainen, T.; Kemell, M.; Heikkilä, M.; Sipi, M.; Kilpeläinen, I. *Packag. Technol. Sci.* **2011**, *24* (4), 249–258.

(6) Mikaeili, F.; Gouma, P. I. *Sci. Rep.* **2018**, *8* (1), 1–8.

(7) Leppänen, I.; Vikman, M.; Harlin, A.; Orelma, H. *J. Polym. Environ.* **2020**, *28* (2), 458–470.

(8) Puls, J.; Wilson, S. A.; Hölter, D. Springer March 20, **2011**, pp 152–165.

(9) Saito, T.; Isogai, A. *Ind. Eng. Chem. Res.* **2007**, *46* (3), 773–780.

(10) Lu, C.; Rosencrance, S.; Swales, D.; Covarrubias, R.; Hubbe, M. A. *Dry Strength: Strategies for Stronger Paper*.

(11) John-louis Flavio, B. DI; Eng, B. *THE WET ADHESION OF POLYVINYLAMINE TO CELLULOSE*.

(12) Parvin, F.; Rahman, M. A.; Islam, J. M. M.; Khan, M. A.; Saadat, A. H. M. In *Advanced*

Materials Research; 2010; Vol. 123–125, pp 351–354.

(13) Ke, T.; Sun, S. X.; Seib, P. *J. Appl. Polym. Sci.* **2003**, *89* (13), 3639–3646.

(14) Ali Akbari Ghavimi, S.; Ebrahimzadeh, M. H.; Solati-Hashjin, M.; Abu Osman, N. A. *J. Biomed. Mater. Res. - Part A* **2015**, *103* (7), 2482–2498.

(15) Xu, H.; Canisag, H.; Mu, B.; Yang, Y. ACS Sustainable Chem. Eng. **2015**, 3, 11, 2631–2639

(16) Plappert, S. F.; Quraishi, S.; Pircher, N.; Mikkonen, K. S.; Veigel, S.; Klinger, K. M.; Potthast, A.; Rosenau, T.; Liebner, F. W. *Biomacromolecules* **2018**, *19* (7), 2969–2978.

(17) Rhim, J. W.; Gennadios, A.; Weller, C. L.; Carole Cezeirat; Hanna, M. A. *Ind. Crops Prod.* **1998**, *8* (3), 195–203.

(18) Dou, Y.; Zhang, B.; He, M.; Yin, G.; Cui, Y.; Savina, I. N. *Polymers (Basel).* **2015**, *7* (3), 580–591.

(19) Soni, R.; Asoh, T. A.; Uyama, H. *Carbohydr. Polym.* **2020**, *238*, 116203.

(20) Soni, R.; Asoh, T. A.; Hsu, Y. I.; Shimamura, M.; Uyama, H. *Polym. Degrad. Stab.* **2020**, *177*, 109165.

(21) Sun, B.; Hou, Q.; Liu, Z.; Ni, Y. *Cellulose* **2015**, *22* (2), 1135–1146.

(22) Abdul Khalil, H. P. S.; Davoudpour, Y.; Islam, M. N.; Mustapha, A.; Sudesh, K.; Dungani, R.; Jawaid, M. *Carbohydrate Polymers*. **2014**, pp 649–665.

(23) Zhang, H.; Liu, P.; Musa, S. M.; Mai, C.; Zhang, K. *ACS Sustain. Chem. Eng.* **2019**, *7* (12), 10452–10459.

(24) Kimura, S.; Isobe, N.; Wada, M.; Kuga, S.; Ko, J. H.; Kim, U. J. *Carbohydr. Polym.* **2011**,

83 (4), 1850–1853.

(25) Kim, U. J.; Isobe, N.; Kimura, S.; Kuga, S.; Wada, M.; Ko, J. H.; Jin, H. O. *Polym. Degrad. Stab.* **2010**, *95* (12), 2277–2280.

Concluding Remarks

In this doctoral thesis, cellulose nanofiber reinforced starch film prepared that possess adequate wet strength, water durability, and marine degradability.

In chapter 1, TCNF/starch film prepared with 60% cellulose nanofiber/40% starch composite (1:0.6 weight ratio) showed minimum swelling with adequate wet strength. The addition of starch promoted the interaction between TCNF and starch through hemiacetal bonding. Furthermore, effects of mixing three different kinds of starch: (hydroxypropyl starch (HPS), acetyl starch (AS), and acetyl oxidize starch (AOS)) with TCNF, on swelling and wet strength properties of TCNF/modified starch film had comprehensively studied. AS and AOS have lesser hydroxyl moieties than HPS, so less crosslinking density causes higher swelling and lower wet strength. The highest wet strength and minimum swelling were observed with TCNF/HPS film.

In chapter 2, the effect of starch paste storage time on the optical, mechanical, and water resistance properties of TCNF/starch films were analyzed. Short-term storage of starch pastes was found to improve the mechanical and water resistance properties of TCNF/starch films, owing to the synergistic effect of starch paste crystallinity and hemiacetal crosslinking. However, the long-term storage of starch pastes promoted granules that reduced hemiacetal crosslinking density and negatively affected the film properties. Moreover, effect of modified starch reassociation on water durability of TCNF/modified starch films were comparatively analyzed. Further, TCNF/HPS film prepared with 3 days stored HPS paste was found to show the most acceptable dried and wet film properties. In addition, TCNF/HPS film showed higher marine microbial degradability compare to neat TCNF film. These results suggest that mixing of reassociated starch paste not only enhanced the film properties also elevated microbial degradability.

In chapter 3, the freshwater durability and marine degradability of oxidized cellulose nanofiber (OMCNF) films were investigated. Sodium periodate oxidation was optimized to introduce aldehyde moieties on cellulose nanofiber surface and to get adequate mechanical properties of OMCNF film. The OMCNF film prepared with 176 µmol/g aldehydes (1 h oxidation at 28 °C) shown adequate mechanical properties in dried and wet conditions. Further, the film water durability could be enhanced by the addition of starch (HPS). The formation of hemiacetal crosslinking between oxidized cellulose nanofiber and starch elevated water durability of OMCNF/HPS film. Moreover, starch addition enhanced microbial growth that increased OMCNF/HPS film's degradability in marine conditions.

In conclusion, the technique developed in this thesis extends the usages of polysaccharides-based films in packaging. TCNF/starch film and OMCNF/starch film are expected to not only contribute significantly to a reduction in the amount of new marine debris deposited globally but also to a more efficient and sustainable material cycling process and the reduction of greenhouse gases, giving it the potential to enable the realization of the United Nation’s Sustainable Development Goals. The author believes that the TCNF, OMCNF reinforced starch films open the research for the next generation renewable, biodegradable, water durable high performance - green packaging.

List of Publications

1. Cellulose Nanofiber Reinforced Starch Membrane with High Mechanical Strength and Durability in Water

Raghav Soni, Taka-Aki Asoh*, and Hiroshi Uyama*

Carbohydrate Polymers, **2020**, *238 (116203)*.

DOI: 10.1016/ j.carbpol.2020.116203

2. Effect of Starch Retrogradation on Wet Strength and Durability of Cellulose Nanofiber Reinforced Starch Film

Raghav Soni, Taka-Aki Asoh*, Yu-I Hsu, Michiyo Shimamura and Hiroshi Uyama*

Polymer Degradation and Stability, **2020**, 177 (*109165*).

DOI: 10.1016/j.polymdegradstab.2020.109165

3. Synergistic Effect of Hemiacetal Crosslinking and Crystallinity on Wet Strength of Cellulose Nanofiber Reinforced Starch Films

Raghav Soni, Yu-I Hsu, Taka-Aki Asoh*, and Hiroshi Uyama*

Food Hydrocolloids

DOI: 10.1016/j.foodhyd.2021.106956

4. A Facile Method to Prepare Fresh Water Durable and Marine Degradable Cellulose Nanofiber Reinforced Starch Film

Raghav Soni, Yu-I Hsu, Taka-Aki Asoh*, and Hiroshi Uyama*

In Preparation

Acknowledgement

This study was carried out from 2018 to 2021 at Department of Applied Chemistry, Graduate School of Engineering, Osaka University. During this fantastic experience in the doctoral 3 years, I have received a lot of invaluable assistance from all people around me. Their support and advices contribute to the accomplishment of the thesis.

First and foremost, I would like to express my deepest gratitude to my supervisor, Prof. Hiroshi Uyama, for his continuous guidance and discussion on my research, and his kind hearted encouragement as well. I also sincerely thanks him for providing opportunities to attend the academic conferences including the internal and international, by which my views were broadened, my knowledge was expanded and my ability was improved. His keen and vigorous academic observations enlighten me in my future study and career.

Besides my advisor, I would like to thanks rest of my thesis committee : Prof. Masaya Nogi and Prof. Norimistu Tohnai, for their insightful comments and their donation of time.

I am profoundly grateful to Assoc. Prof. Taka-Aki Asoh, for his suggestions and inspirations to improve the quality of my research. His novel insight and knowledge sharing promoted my thesis accomplishment. I also deeply thanks him for the research guidance and manuscript revising. Without his support, my doctoral thesis cannot be finished smoothly.

I appreciate Assist. Prof. Yu-I Hsu for her discussions and advices about my subject at any time and the knowledge sharing. I also thanks her for suggestions and revisions.

I grateful to Dr. Michiyo Shimamura, Japan Agency for Marine-Earth Science and Technology (JAMSTEC) for performing marine degradation test.

I would like to express my gratitude to Nihon shokuhin kako Co. Ltd. for providing starch samples.

I am highly grateful to Ms. Yoko Uenishi and Mrs. Tomoko Shimizu for kind help and warm-hearted support.

I am very thankful to the past and present fellow lab mates in Uyama Lab: Dr. Yasushi Takeuchi, Dr. Masatoshi Kato, Dr. Chen Qian, Dr. Zhengtian Xie, Dr. Jia Yankun, Dr. Toshiki

Tamiya, Dr. Shunsuke Mizuno, Mr. Naharullah Bin Jamaluddin, Ms. Hanyu Wen, Ms. Yanting Lyu, Mr. Akihide Sugawara, Mr. Mark Adam Malaluan Ferry, Mrs. Wang Yan, Mr. Zhang Lu Wei, Ms. Wei Meng, Mr. Yuxiang Jia, Mr. Emil Hajili, Mrs. Madhurangika Panchabashini Horathal Pedige, Ms. Qian Jin, Ms. Yiying Wang, Ms. Lulu Huang, Ms. Jiaxin Chen, Ms. Zeying Cao, Ms. Xuran Guo, Ms. Linxiuan Li, Ms. Megumi Nakamura, Ms. Anna Shigaki, Mr. Ginga Hoshi, Mr. Toshiki Honda, Mr. Tatsuya Yamamoto, Ms. Airi Ozaki, Ms. Shiho Takai, Mr. Yuya Fujiwara, Mr. Yuka Kashihara, Mr. Kohei Kikkawa, Mr. Yuji Kiba, Mr. Atsusi Koizumi, Mr. Yuki Shioji, Ms. May Myat Noe, Ms. Hasinah Binti Mohamed Rafiq, Mr. Takeshi Hiraoka, Mr. Motoi Oda, Mr. Kaita Kikuchi, Mr. Koki Tsujita, Mr. Hajime Fujimori, Ms. Suzune Miki, Ms. An Thuy Le Huynh, etc. for their kind-hearted help both in my research and daily life.

I am very grateful to Mr. Shibu Chameettachal, Ms. Sriya Yeleswarapu, Ms. Soumya Sethi for their motivation, guidance and support. I am appreciate Mr. Pardeep Kumar, Mr. Brijesh sharma, Mr. Ravi Yadav, Mr. Vaibhav bansode, Mr. Sumit Pal, Mr. Harendra Kumar, Mr. Ritesh Mishra etc, for their help and support.

The financial support from Japan International Corporation Agency (JICA) for my academic study and my stay in Japan is greatly appreciated.

Last but not least, I would like to express appreciation to my parents and family members for their warm encouragement to pursue research, endless support and love throughout my life.

July 2021

Raghav Soni